Journal for ImmunoTherapy of Cancer

A very long-acting IL-15: implications for the immunotherapy of cancer

John A Hangasky ,[1] Wei Chen,[2] Sigrid P Dubois,[2] Anusara Daenthanasanmak,[2] Jürgen R Müller,[2] Ralph Reid,[1] Thomas A Waldmann ,[2] Daniel V Santi[1]

To cite: Hangasky JA, Chen W, Dubois SP, *et al*. A very long-acting IL-15: implications for the immunotherapy of cancer. *Journal for ImmunoTherapy of Cancer* 2022;**10**:e004104. doi:10.1136/jitc-2021-004104

► Additional supplemental material is published online only. To view, please visit the journal online (http://dx.doi.org/10.1136/jitc-2021-004104).

TAW and DVS contributed equally.
WC, SPD and AD contributed equally.

Accepted 14 December 2021

[1]ProLynx Inc, San Francisco, California, USA
[2]Lymphoid Malignancies Branch, Center for Cancer Research, National Cancer Institute, Bethesda, Maryland, USA

Correspondence to
Dr Daniel V Santi;
Daniel.v.santi@prolynxinc.com

ABSTRACT

Background Interleukin-15 (IL-15) is an important cytokine necessary for proliferation and maintenance of natural killer (NK) and CD8$^+$ T cells, and with great promise as an immuno-oncology therapeutic. However, IL-15 has a very short half-life and a single administration does not provide the sustained exposure required for optimal stimulation of target immune cells. The purpose of this work was to develop a very long-acting prodrug that would maintain IL-15 within a narrow therapeutic window for long periods—similar to a continuous infusion.

Methods We prepared and characterized hydrogel microspheres (MS) covalently attached to IL-15 (MS~IL-15) by a releasable linker. The pharmacokinetics and pharmacodynamics of MS~IL-15 were determined in C57BL/6J mice. The antitumor activity of MS~IL-15 as a single agent, and in combination with a suitable therapeutic antibody, was tested in a CD8$^+$ T cell-driven bilateral transgenic adenocarcinoma mouse prostate (TRAMP)-C2 model of prostatic cancer and a NK cell-driven mouse xenograft model of human ATL (MET-1) murine model of adult T-cell leukemia.

Results On subcutaneous administration to mice, the cytokine released from the depot maintained a long half-life of about 168 hours over the first 5 days, followed by an abrupt decrease to about ~30 hours in accordance with the development of a cytokine sink. A single injection of MS~IL-15 caused remarkably prolonged expansions of NK and γδ T cells for 2 weeks, and CD44^{hi}CD8$^+$ T cells for 4 weeks. In the NK cell-driven MET-1 murine model of adult T-cell leukemia, single-agent MS~IL-15$_{50\ \mu g}$ or anti-CCR4 provided modest increases in survival, but a combination—through antibody-depedent cellular cytotoxicity (ADCC)—significantly extended survival. In a CD8$^+$ T cell-driven bilateral TRAMP-C2 model of prostatic cancer, single agent subcutaneous MS~IL-15 or unilateral intratumoral agonistic anti-CD40 showed modest growth inhibition, but the combination exhibited potent, prolonged bilateral antitumor activity.

Conclusions Our results show MS~IL-15 provides a very long-acting IL-15 with low C_{max} that elicits prolonged expansion of target immune cells and high anticancer activity, especially when administered in combination with a suitable immuno-oncology agent.

INTRODUCTION

Interleukin-15 (IL-15) is a ~14 kDa protein belonging to a family of interleukins that use a common cytokine-receptor γ-chain. IL-15 is essential for the proliferation, maintenance, and survival of natural killer (NK) and CD8$^+$ T cells, and recombinant human IL-15 (rhIL-15, hereafter referred to as IL-15) is of major interest as an immuno-oncology agent.[1–5] This pleiotropic cytokine stimulates immune cell responses through the same dimeric IL-2Rβ/γc receptor complex as IL-2 (figure 1) but the two cytokines exhibit functionally distinct activities associated with their unique Rα subunits.[6] IL-15 is expressed in association with its high-affinity IL-15Rα receptor chain on the surface of monocytes and dendritic cells and is predominately trans-presented to target immune cells to form a high-affinity IL-15/IL-15Rα/IL-2Rβ/γc complex[7 8]; in addition, to a lesser extent free soluble IL-15 can act in cis on dimeric and trimeric receptors. IL-2 binds with moderate affinity to the same IL-2Rβ/γc receptor complex and with high affinity to the IL-2Rα/IL-2Rβ/γc trimeric receptor found on regulatory T cells. Thus, both IL-15 and IL-2 bind to and stimulate NK and CD8$^+$ T cells, but regulatory T cells are predominately stimulated by IL-2. Moreover, in contrast to IL-2, IL-15 inhibits activation-induced cells death, which leads to memory cell survival.[9] Although IL-15 has modest anticancer activity as a single agent, it shows significant effects in combination with other immuno-oncology agents and it is in this setting that IL-15 is expected to be efficacious.[3]

NK and memory T-cell proliferation requires IL-15 exposure at a level above a threshold concentration for a protracted period—a critical 'time-over-target'.[10–12] However, IL-15 has a short $t_{1/2}$—only ~2.5 hours in humans—and the high dose of a single injection necessary to achieve adequate sustained exposure is accompanied by a high C_{max} and associated toxicities.[13] Hence, extensive efforts have been expended to develop potent, long-acting IL-15 receptor agonists in which a single dose maintains the agonist in a narrow therapeutic window for a long period. The most common approaches employed to

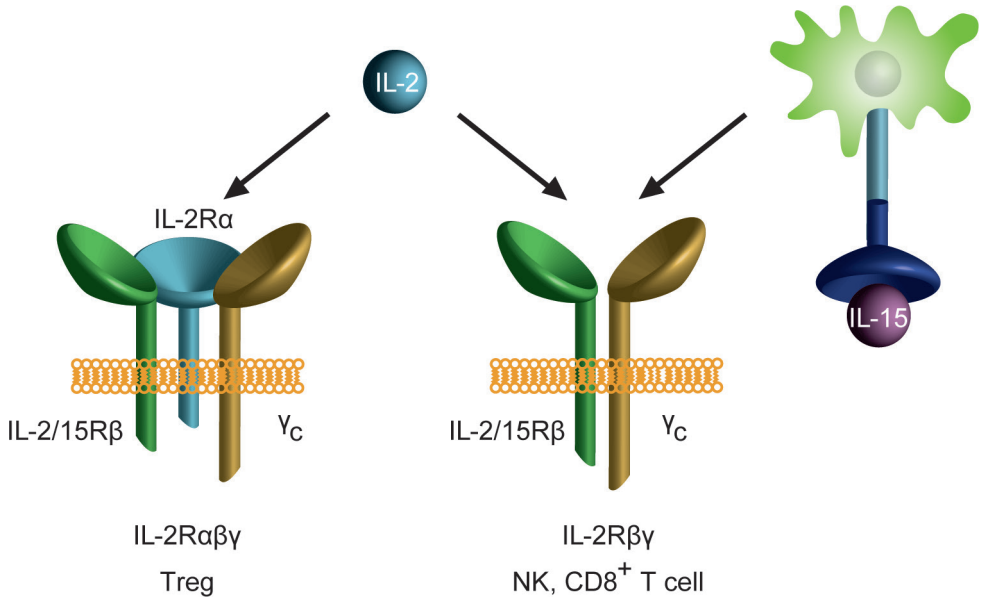

Figure 1 Interleukin (IL)-15 and IL-2 receptor specificities. IL-15 is trans-presented in association with IL-15Rα to IL-2Rβ/γc receptor also used by IL-2. IL-2 binds moderately to cells with the same IL-2Rβ/γc receptor, and with high affinity to the trimeric IL-2Rα/IL-2Rβ/γc receptor on regulatory T (Treg) cells. NK, natural killer.

increase the $t_{1/2}$ of IL-15 involves increasing the molecular size to reduce the renal elimination rate and/or by targeting the neonatal Fc receptor (FcRn). These include incorporation of part of the IL-15Rα and/or attachment to polyethylene glycol (PEG), Fc, or serum albumin to the cytokine, and are exemplified by Alt-803 (IL-15 N72D/IL-15Rα-Fc), hetIL-15 (IL-15/IL-15Rα), RLI (single chain fusion of IL-15 and IL-15$Rα_{sushi}$), and NKTR-255 (PEGylated IL-15).[14] Enigmatically, although the half-life extension technologies used often lengthen the $t_{1/2}$ of a protein to a week or longer in humans, the IL-15 agonists studied have systemic elimination $t_{1/2}$s of not longer than 1 day and usually only several hours.[14] Another approach to maintain a constant level of IL-15 for a prolonged period is continuous intravenous infusion (CIV). Here, 5-day[15] or 10-day[16] CIV of IL-15 showed remarkable increases of $CD8^+$ T cells, NK cells, and $CD56^{bright}$NK cells. Regardless, CIV administration is an impractical route of administration, and it is desirable to have an effective IL-15 agonist possessing the convenience and acceptance of a single subcutaneous injection of once weekly or longer intervals.

We have developed a general approach for half-life extension of therapeutics in which the pharmacokinetics (PK) of the circulating drug can mimic a continuous infusion. As previously described,[17 18] a drug is covalently tethered to a long-lived carrier by a linker that slowly cleaves by β-elimination to release the free drug (figure 2). The base-catalyzed first-order cleavage rate of the linker is controlled by the nature of an electron-withdrawing 'modulator' (Mod), which regulates the acidity of an adjacent carbon-hydrogen bond. These linkers are not affected by enzymes and are extraordinarily stable when stored at low pH and temperature.[17 19] One carrier we use is a mesoporous tetra-PEG hydrogel.[18 20] These hydrogels—fabricated as uniform ~60 µm microspheres (MS)[20]—are injected subcutaneously through a small-bore needle where they serve as a stationary, localized depot to slowly release the drug to the systemic circulation. We also incorporate slower cleaving β-eliminative linkers in crosslinks of these polymers, so gel degradation occurs in vivo after drug release.[18 21]

The primary objective of this work was to develop a very long-acting IL-15. First, we describe the synthesis and characterization of an MS~IL-15 prodrug. Next, we describe the PK of the conjugate in mice, and show a very long half-life and low C_{max} of the released cytokine. Then, we describe the remarkably long-lasting effects of subcutaneous MS~IL-15 on the proliferation and expansion of NK and $CD8^+$ T cells. Finally, we demonstrate potent antitumor activity of MS~IL-15 in combination with anti-CCR4

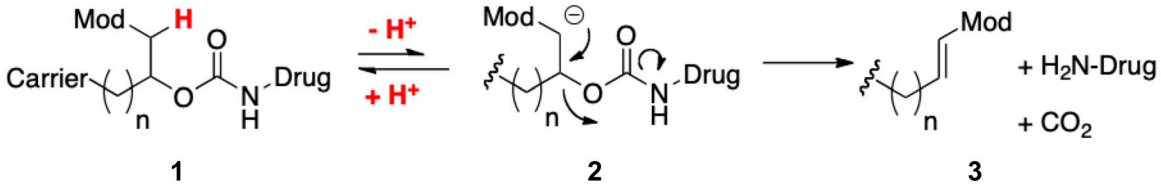

Figure 2 β-Eliminative drug release. Mod, modulator.

in the MET-1 model of adult T-cell leukemia (ATL), and in combination with intratumoral (IT) agonistic anti-CD40 in the bilateral TRAMP-C2 model of prostatic cancer.

MATERIALS AND METHODS

The following are materials and methods used in this work. Complete details of chemical syntheses and characterization, PK and pharmacodynamic (PD) experiments, and therapeutic studies are provided in online supplemental information.

Materials

IL-15 (>95% pure) was provided by the National Cancer Institute. Receptor-linked interleukin-15 (RLI) was produced at ATUM (Newark, California) as reported.[22] Mogamulizumab-kpkc (NDC code 42747-761-01) was obtained from the NIH Pharmacy. Anti-CD40 (#BP0016-2) was obtained from BioXCell (Lebanon, New Hampshire). C57B/6J plasma was purchased from Innovative Research (Novi, Michigan). All other chemicals and reagents were purchased from commercial vendors unless otherwise stated.

Preparation of MS~IL-15

As described,[23] azido-linker-IL-15 was prepared by conjugating N_3-PEG_4-Linker($MeSO_2$)-CHO to the IL-15 via reductive alkylation using $NaCNBH_3$. Excess reagents were removed using a PD-10 column (GE Healthcare). Then, the azido-linker-IL-15 was attached to BCN-derivatized MS through strain promoted azide-alkyne cycloaddition. The unreacted BCN groups were capped with N_3-PEG_7 (Sigma-Aldrich). The MS~IL-15 slurry was washed and equilibrated with 25 mM citrate, pH 6.0, 500 mM NaCl, and 0.05% tween-20 containing 30 mM Met as an anti-oxidant and stored at 4°C.

In vitro characterization of MS~IL-15

The release kinetics of MS~IL-15 were determined under accelerated release conditions as previously described.[18 20] The purity of IL-15 on the MS was determined by monitoring the released proteins at pH 9.4, 37°C using high-performance liquid chromatography (HPLC). The bioactivity of $^{\alpha}$N-aminopropyl-IL-15 (IL-15_{AP}) was assessed using the U2OS cell-based assay kit for IL-2Rβγ binding (DiscoverX, Part #93-0998E3CP5).

Pharmacokinetics of MS~IL-15 in immunocompetent mice

Dosing solutions were prepared by diluting the MS~IL-15 slurry in 25 mM Na citrate buffer pH 6.0 containing 500 mM NaCl, 0.05% tween-20, and 1.25% (w/v) hyaluronic acid. Syringes with fixed needles (27 G) were backfilled with the MS~IL-15 conjugate (50 µg IL-15, 100 µL). The contents of the syringes were administered subcutaneously to normal, male C57BL/6J mice or NOD scid gamma (NSG) mice. Blood samples were collected in EDTA collection tubes, containing HALT protease inhibitor, over a predefined time course from alternating groups of mice (n=3/group). Plasma was prepared and stored at –80°C until analysis. The rhIL-15 concentrations in serum were assessed using a hIL-15-specific ELISA (R&D Systems, hIL-15 Quantikine) performed according to the manufacturer's instructions.

Pharmacodynamics of MS~IL15

Normal, male C57BL/6J mice (n=3–5/group) received either a single injection of MS~IL-$15_{50\ \mu g}$ subcutaneously or one to five injections of rhIL-15 (5–50 µg) intraperitoneally. On days 2, 5, 7, 14, 21, and 28, mice were bled or sacrificed. Blood, splenocytes, and lymph node lymphocytes were immunophenotyped to quantitate NK cells, B cells, $CD4^+$, $CD8^+$, $CD44^{hi}CD8^+$, γδ T cells, and $Ki67^+$ cells. Untreated mice were used to determine baseline cell numbers.

Flow cytometry

Peripheral blood mononuclear cells (PBMCs) were prepared using ammonium-chloride-potassium (ACK) lysis buffer and incubated with a fixable viability dye to label dead cells. The FcRγII/II receptor was then blocked using CD16/32 (2.4G2) (BD Biosciences). PBMCs were surface stained using optimal Ab concentrations and fixed for intracellular staining following protocols from the eBioscience Foxp3/Transcription Factor Staining Buffer Set (online supplemental table S1). Stained single cell suspensions were analyzed on either FACScan (BD Biosciences) or Attune NxT flow cytometer (Thermofisher) and data were analyzed using FlowJo cytometry analysis software (TreeStar, Ashland, Oregon).

TRAMP-C2 model

The TRAMP-C2 cell line, derived from a prostate tumor of the TRAMP mouse, was administered to four groups of wild-type C57BL/6J mice on both flanks. Following reported methods[24] when the tumors volumes reached 40–60 mm^3, treatment began. Mice were treated with either empty MS, anti-CD40, MS~IL-$15_{50\ \mu g}$, or the combination of MS~IL-$15_{50\ \mu g}$ and anti-CD40. Measurements of the right and left tumors were obtained from caliper measurements. Kaplan-Meier mouse survival plots were generated based on the mouse survival, monitored based on humane end point criteria.

MET-1 murine model of ATL

The MET-1 cell line was established from the peripheral blood collected from a patient with acute ATL.[25] The ATL leukemia model MET-1 was established by the intraperitoneal injection of 2×10^7 MET-1 cells into severe combined immunodeficient/non-obese diabetic (SCID/NOD) wild-type mice as described previously.[25 26] Treatment began when the sIL-2Ra levels were >1000 pg/mL serum. MS~IL-$15_{50\ \mu g}$ was administered to mice subcutaneously. On day 10, sIL-2Rα levels were quantitated using a human CD25/IL-2Rα Quantikine ELISA kit (R&D Systems, DR2A00) following manufacturer's instructions. Kaplan-Meier mouse survival plots were generated based on the survival of mice in each group.

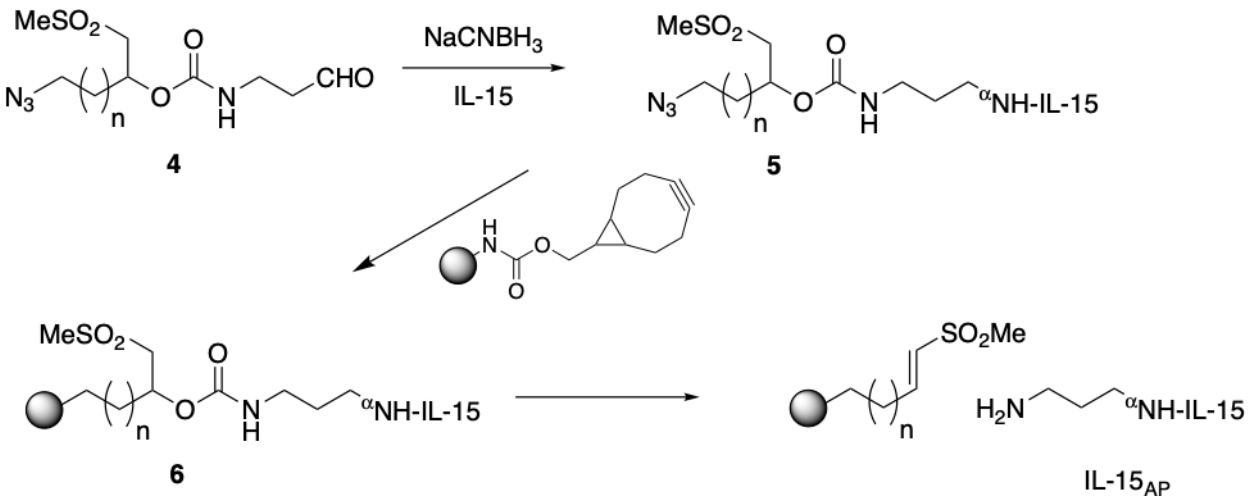

Figure 3 Synthesis of MS~IL-15 and IL-15_{AP} release. IL, interleukin; IL-15_{AP}, $^{\alpha}$N-aminopropyl-IL-15; MS, microspheres.

Statistical analysis

Statistical testing was performed using GraphPad Prism V.9. Values are presented as mean±SD, unless otherwise stated, and are reported in the text and figure legends. In all cases, values of p<0.05 were regarded as statistically significant.

RESULTS

Preparation and characterization of MS~IL-15

We prepared the MS~IL-15 conjugates by a reported method for site-specific attachment of macromolecular carriers to the N-terminus of proteins[23] (figure 3). Amine-derivatized MS, prepared from 4-arm $PEG_{20\ kDa}$ prepolymers and containing a β-eliminative linker in all crosslinks for programmed biodegradation,[20] served as the macromolecular carrier. First, we determined the optimal ratio of N_3-linker-aldehyde 4 (Mod $MeSO_2$–) to rhIL-15 that gave the highest balanced yield of monoalkylated N_3-linker-IL-15, 5 (online supplemental figure S1). A PEG-shift sodium dodecyl sulfate-polyacrylamide gel electrophoresis assay of the optimized reaction mixture[23] showed ~45% unreacted IL-15, ~55% IL-15 having one linker and ≤5% with more than one linker; thus, ≥90% of the product was the desired monoalkylated IL-15. Then, the N_3-linker-IL-15, 5, was coupled to BCN-modified MS by strain-promoted alkyne-azide cycloaddition, and unreacted 5 and free IL-15 were washed from the particulate MS to give the MS~IL-15 containing ~5 mg IL-15/mL gel slurry.

Base catalyzed β-elimination of the MS~IL-15 resulted in complete release of N^{α}-amino-propyl IL-15 (IL-15_{AP}) with $t_{1/2}$ 1030 hours, in agreement with previous results using the same linker.[23] The purity of IL-15_{AP} on the MS~IL-15 conjugate was assessed by HPLC quantitation of released proteins versus time at pH 9.4; when extrapolated to t=0, ≥95% of the protein on MS analyzed as IL-15_{AP} (online supplemental figure S2). In accordance with the high stability of linkers at low pH and temperature,[17 19] after 1 month of storage at pH 6.0, 4°C, the purity of IL-15 on the MS remained >92% (online supplemental figure S2B). Finally, the half maximal effective concentration (EC_{50}) of IL-15_{AP} released from the MS~IL-15 at pH 7.4 over 10 days was the same (95% CI) as native IL-15 in both an IL-2Rβ/γc dimerization cell-based assay and CTLL-2 cell proliferation assay, demonstrating that IL-15_{AP} released from MS is equipotent to native IL-15 (online supplemental figure S3).

Stability of IL-15

Successful use of MS~IL-15 requires that the attached IL-15 be stable in the subcutaneous space and under storage conditions. Asn77 of IL-15 undergoes deamidation with a $t_{1/2}$ of ~4 days at pH 7.4, 37°C, but the IL-15(Asp77) product is equipotent in the CTLL-2 bioassay and <5% additional degradation occurred over 8 days.[27 28] Here, when IL-15 was kept at pH 7.4, 37°C, for 10 days, there was no significant change in EC_{50} in cell-based IL-2Rβ/γc dimerization or ELISA assays (online supplemental figure S4). At storage conditions at pH 6.0, 4°C, Asn77 deamidation is very slow[27] and we observed no significant change in the EC_{50} of IL-15 over 28 days using the cell-based assay (online supplemental figure S5). Hence, the IL-15 of MS~IL-15 is sufficiently stable to withstand conditions expected in the subcutaneous space and for long-term storage.

Pharmacokinetics of MS~IL-15

The concentration versus time plot of IL-15_{AP} released from a single subcutaneous dose of MS containing 50 µg IL-15, designated as MS~IL-$15_{50\ µg}$, in C57BL/6J mice is shown in figure 4. We chose a standard dose of MS~IL-$15_{50\ µg}$ because it provides a plasma concentration in mice similar to the ~200 to 300 pM effective plasma level attained in CIV IL-15 in monkeys[29] and man.[16] As shown, IL-15_{AP} released from MS~IL-$15_{50\ µg}$ eliminates with a $t_{1/2}$ of ~168 hours over ~120 hours which then abruptly decreases to a $t_{1/2}$ ~30 hours, both significantly longer than other IL-15 agonists (table 1). When a second dose of MS~IL-$15_{50\ µg}$ was administered on day

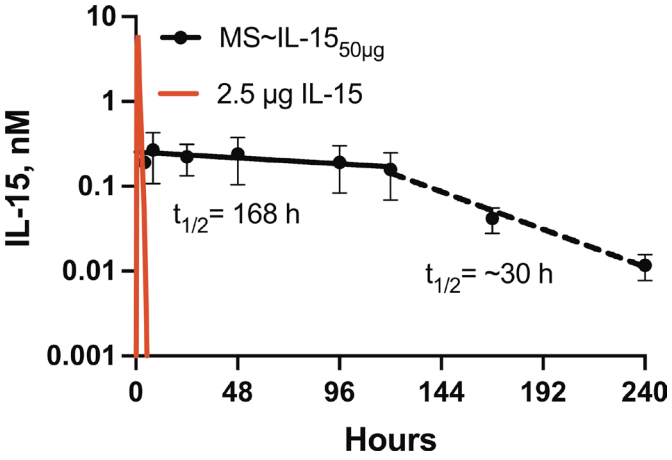

Figure 4 C versus t plot of IL-15$_{AP}$ released from MS~IL-15. Mice (n=3/group) were administered MS~IL-15$_{50\ \mu g}$ on day 0 (●). The red line depicts the C versus t of 2.5 µg IL-15 administered intraperitoneally that has a $t_{1/2}$ ~0.5 hour. Points are mean±SD. IL, interleukin; IL-15$_{AP}$, $^{\alpha}$N-aminopropyl-IL-15; MS, microspheres.

10 to mice previously treated with MS~IL-15$_{50\ \mu g}$, the $t_{1/2}$ was the ~30 hours observed in the second phase (online supplemental figure S6A). Using the area under the curve $(AUC)_{\infty}$ of IL-15$_{AP}$ released from of MS~IL-15$_{50\ \mu g}$ determined from C versus t plots (n=6), the reported clearance (CL) of 49 mL/hour for IL-15[30] and the eq. $F=AUC_{\infty}\bullet CL/dose$, we calculated a bioavailability of 66%±12%. With the NSG mouse—deficient in the γc receptor and mature immune cells—the C versus t plot after a single dose of MS~IL-15$_{50\ \mu g}$ showed a single $t_{1/2}$ of 200 hours over 24 days (online supplemental figure S6B). Hence, the unusual biphasic PK in normal mice is likely due to one or more classes of immune cells that are deficient in the NSG mouse.

Potential causes of the biphasic PK are (a) the formation of antidrug antibodies (ADAs) and/or (b) an IL-15-induced 'cytokine sink' that increases with target immune cell proliferation and results in increased consumption/CL of IL-15.[14 16 31] We considered ADAs improbable since identical biphasic C versus t plots were observed in each of ~40 mice examined over the course of this work; such uniform occurrence and timing of ADA production is not an expected phenomenon. We also tested for the presence of ADAs using a bridging ELISA[13] (online supplemental figure S7). Mice were injected with MS~IL-15$_{50\ \mu g}$ and plasma was analyzed at day 10 (n=12); then, after a second injection of MS~IL-15$_{50\ \mu g}$ at day 10 plasma was analyzed at day 17 (n=12). Both time points were sampled during the rapid CL phase when IL-15 was at a non-interfering ~10 pM, so if ADAs contributed to CL, they should be present and detectable. All assayed samples were below the detectable level of ~1.3 nM of the control monoclonal antibody (mAb. Hence, it appears likely that the rapid CL phase is due to a cytokine sink that increases with proliferation of IL-15 target immune cells[14]; enigmatically, once formed at day 6, the putative sink appears to be stable to at least day 17.

Pharmacodynamic effects of MS~IL-15$_{50\ \mu g}$ and dose equivalent 5 µg IL-15 once a day×5

With few exceptions,[32] IL-15 PD effects on immune cell expansion in mice have been quantified by single measurements a short time after administration. While single measurements may suffice for agonists with short half-lives, they do not capture the duration or extent of response elicited by multiple administrations or an agonist with a long half-life. Also, they can be misleading when used to compare effects of different regimens or agonists in cell subtypes that reach maxima at different times. Therefore, initial experiments determined a time course for sampling and demonstrated that empty MS have no significant effect on immune cell expansion over 21-day period (online supplemental figure S8). Figure 5 shows NK and CD8^{+} T cells in spleen, lymph nodes, and PBMCs monitored over a 28-day period after a single injection of MS~IL-15$_{50\ \mu g}$ and 5 µg IL-15 once a day×5 in mice, and complete results are provided in online supplemental figure S9A,B. We estimated the amount of IL-15$_{AP}$ released from MS~IL-15 each day by the eq.

Table 1 Half-lives of IL-15 agonists in mice

IL-15 agonist	Route of administration*	Mouse $t_{1/2}$ hour	Reference
MS~IL-15	Subcutaneous	168 (30†)	This work
MS$_{GDM}$~IL-15	Subcutaneous	50	This work
IL-15	Intravenous	0.64	30
IL-15	Intraperitoneal	0.50	31
RLI (IL-15-IL-15Rα$_{sushi}$)	Intraperitoneal	3	35
hetIL-15 (IL-15/IL-15Rα)	Intraperitoneal	4	53
ALT-803 (IL-15 N72D/IL-15Rα-Fc)	Intravenous and subcutaneous	7.5	54
NKTR-255 (PEG-IL-15)	Intravenous	14	32

*Not all routes of administration have been reported in mice.
†Second phase of C versus t plot.
IL, interleukin; MS, microspheres.

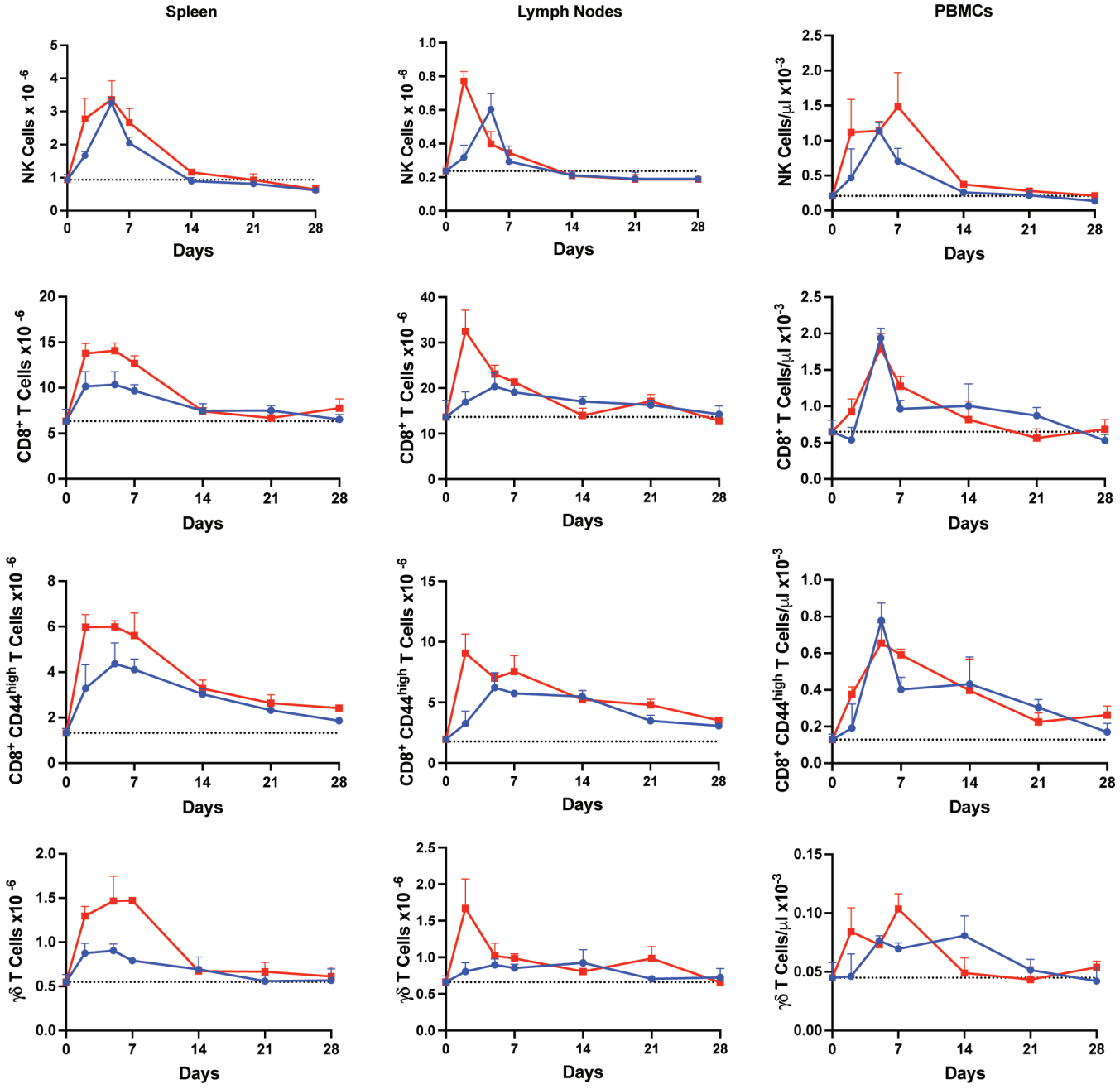

Figure 5 Immune cell expansion by MS~IL-$15_{50\,\mu g}$ over 28 days. Enumeration of NK, $CD8^+$, $CD44^{hi}CD8^+$, and γδ T cells at 0, 2, 5, 7,14, 21, and 28 days in the spleen, lymph nodes, and PBMCs of mice (n=3/point/group) treated with subcutaneous MS~IL-$15_{50\,\mu g}$ (▪) or intraperitoneal 5 µg IL-15 once a day×5 (●). The dotted line represents the mean value of the pretreatment controls (n=5). PBMCs were quantified using complete blood count. Points are mean±SD. IL, interleukin; MS, microspheres; NK, natural killer; PBMC, peripheral blood mononuclear cells.

$d(n)=D\times r^{n-1}(1-r)$, where D is the initial amount of IL-15 in the depot and $r=-(24\,hours)\times\ln 2/t_{1/2}$. In the present case, after injection of MS~IL-$15_{50\,\mu g}$ using a release $t_{1/2}$ of 168 hours, the calculated IL-15_{AP} released over day 1 is 4.7 µg, and on day 5 is 3.2 µg, giving an average IL-15_{AP} released over 5 days of ~4 µg/day.

For analyses of PD effects from cell number versus time plots (figure 5), a horizontal line was created from the pretreatment control value extending to the end of the 28-day study period. The duration of expansion was estimated as the closest measured time point to which the experimental data intersected the control horizontal line. The extent of cell expansion was estimated as the AUC over 28 days ($AUC_{28\,d}$) between the horizontal control and the experimental line. Table 2 tabulates the values for duration and $AUC_{28\,d}$ from figure 5 and online supplemental figure S9A. When preferred, the fold increase of cell expansion can be estimated as the experimental $AUC_{28\,d}$/control $AUC_{28\,d}$ over the time of interest.

Several features of the AUC approach to measure total cell expansion are worthy of note. First, the proliferation $AUC_{28\,d}$ values are deceptively lower than conventionally

Table 2 Duration of immune cell expansion and $AUC_{28\,d}$ in PBMCs, lymph nodes, and spleen

		Predose control, cells*	Duration, day		AUC, cells* day†	
Marker	Tissue	Mean±SD	IL-15 5 µg once a day×5	MS~IL-15$_{50\,\mu g}$	IL-15 5 µg once a day×5	MS~IL-15$_{50\,\mu g}$
NK1.1$^+$	Spleen	0.93±0.16	14	14	10	19
	In	0.24±0.03	14	14	0.71	1.5
	PBMC	0.21±0.04	14	14	5.4	12
CD8$^+$	Spleen	6.34±1.32	14	14	51	82
	In	13.6±3.67	14	14	94	130
	PBMC	0.65±0.16	21	21	8.0	7.1
CD44^{hi}CD8$^+$	Spleen	1.32±0.20	28	28	46	69
	In	1.95±1.85	28	28	70	104
	PBMC	0.13±0.03	28	28	6.5	7.0
TCRγδ$^+$	Spleen	0.55±0.09	14	14	3.9	10
	In	0.66±0.08	14	14	4.2	8.1
	PBMC	0.04±0.01	21	14	0.48	0.48
Ki67$^+$ NK1.1$^+$	Spleen	0.14±0.05	7	7	6.8	6.0
	In	0.05±0.01	7	7	1.1	1.5
	PBMC	0.03±0.01	14	14	2.3	2.5
Ki67$^+$CD44^{hi}CD8$^+$	Spleen	0.47±0.16	7	7	15	18
	In	0.65±0.21	7	7	16	26
	PBMC	0.03±0.01	21	14	1.6	1.1
Ki67$^+$ TCRγδ$^+$	Spleen	0.26±0.05	14	14	3.5	8.6
	In	0.36±0.07	14	14	2.3	6.1
	PBMC	0.020±0.005	21	21	0.54	0.6

*Control values are cells×10^{-6} for spleen and lymph nodes (In), and cells/µL×10^{-3} for PBMCs.
†AUC values are cells×10^{-6}×day for spleen and In, and cells/µL×10^{-3}×day for PBMCs.
AUC, area under the curve; IL, interleukin; MS, microspheres; PBMC, peripheral blood mononuclear cell.

reported because the $AUC_{28\,d}$ of parental cells includes the entire contraction phase; over the period of proliferation, the per cent Ki67$^+$ of NK and CD44^{hi}CD8$^+$ T cells were 70%–90% of the parent (online supplemental figure S9A). Second, $AUC_{28\,d}$ of long-lived subsets, such as CD44^{hi}CD8$^+$ T cells, may be deceptively high because the contraction phase may be longer than that of the parent. Third, with exception of NK cells, the $AUC_{28\,d}$ of target immune cell proliferation and expansion in PBMCs correlated with those from spleen and lymph nodes with R=99.3% and 98.8%, respectively. $AUC_{28\,d}$ of NK cells in PBMCs were ~10-fold higher than expected compared with spleen and lymph nodes, which reduced the correlation; interestingly, NTKR-255 also shows very high expansion of NK cells in peripheral blood.[32] Therefore, T cell expansion in mouse PBMCs can be legitimately used as surrogates to avoid sacrificing mice and performing numerous surgical procedures.

The duration of immune cell expansion of 5 µg IL-15 once a day×5 vs MS~IL-15$_{50\,\mu g}$ in spleen, lymph nodes, and PBMCs are all quite similar, showing ~14 days for NK, CD8$^+$, and γδ T cells, and ~28 days for CD44^{hi}CD8$^+$ T cells. As measured by Ki67$^+$, proliferation of NK, CD8$^+$, and CD44^{hi}CD8$^+$ T cells in all tissues usually peaks at ~2 days then drops to control by 7 days, although proliferation of γδ T cells reaches control levels at 14 days (online supplemental figure S9A). As expected, proliferation of CD44^{low}CD8$^+$-naïve T cells, B cells, and CD4$^+$ T cells were not significant. On average, the $AUC_{28\,d}$ of immune cell proliferation and expansion for MS~IL-15$_{50\,\mu g}$ is ~150% of that for 5 µg IL-15once a day×5.

Frutoso *et al*[33] observed hyporesponsiveness of NK cells but not CD8$^+$ T cells after a second injection of IL-15, RLI, or RLI-Fc. On a second injection of MS~IL-15$_{50\,\mu g}$ 28 days after the first, we also observed low (40%) proliferation of NK cells. CD8$^+$ T cells were not affected when measured at a single time 2 days postadministration as reported,[33] but the $AUC_{28\,d}$ of CD8$^+$ T cells was attenuated by about 50%.

PD effects of single and sequential doses of IL-15 and superagonist RLI

We determined the PD effects in PBMCs after single doses of 5–50 µg IL-15 (figure 6 and online supplemental

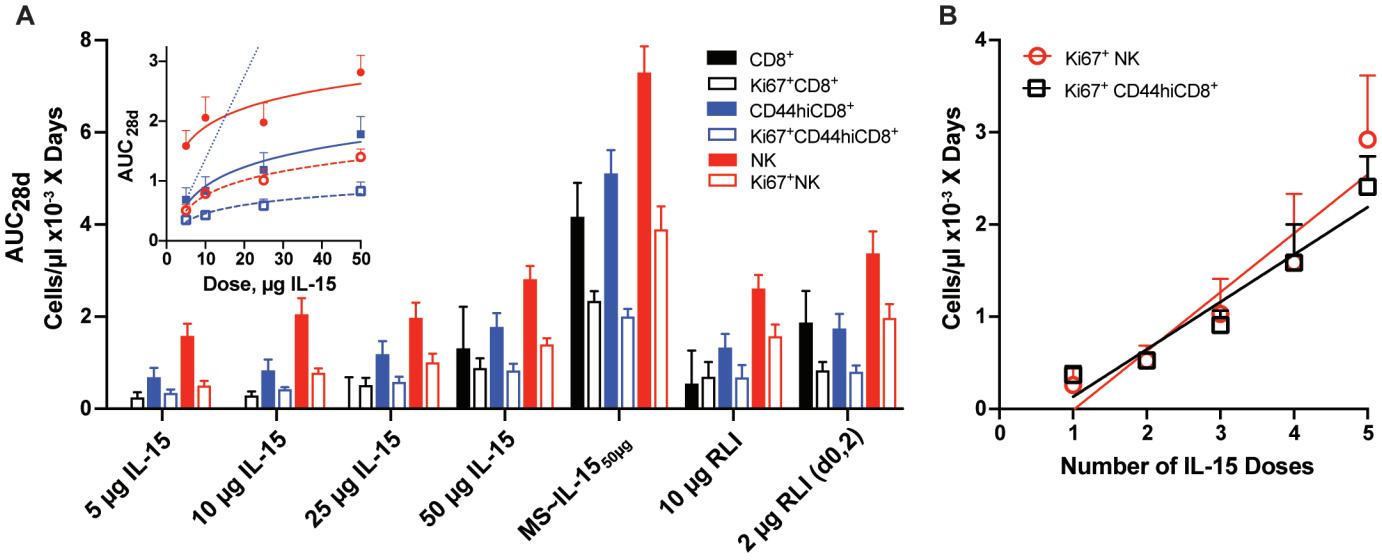

Figure 6 PD effects of single and sequential doses of IL-15 and the super-agonist RLI in PBMCs. (A) $AUC_{28\,d}$ for PD effect on target immune cells. Mice (n=4–5/group) were administered single intraperitoneal doses of 5–50 µg IL-15, 10 µg RLI, MS~IL-$15_{50\,\mu g}$, or two doses of 2 µg RLI separated by 48 hours. PBMCs were collected over 28 days, and target immune cells analyzed for duration and $AUC_{28\,d}$. Inset: $AUC_{28\,d}$ vs IL-15 dose for NK (●), $Ki67^+$ NK (◯), $CD44^{hi}CD8^+$ (■), and $Ki67^+$ $CD44^{hi}CD8^+$ (□). Data points are fitted to the logarithmic equation derived in SI. Here, the relative fold-change in time-over-target with an X-fold increase in dose=1+ln(X)/ln($dose_1/C_{min}V_d$). The dotted line shows the trace for the $CD44^{hi}CD8^+$ T cell dose response when the response between 0 and 5 µg IL-15 is used to define a linear slope. (B) PD effects of IL-15 after subcutaneous administration of 5 µg to mice (n=5/group) on d0, then sequentially each day on d0-1, d1-2, d1-3, and d1-4. Analysis of $AUC_{28\,d}$ of $Ki67^+$ proliferating NK and $CD44^{hi}CD8^+$ T cells in PMBCs began on d0. Cell numbers were directly measured using an Attune NxT. Data show the mean±SD of the $AUC_{28\,d}$ for individual mice. AUC, area under the curve; IL, interleukin; MS, microspheres; NK, natural killer; PBMC, peripheral blood mononuclear cells; PD, pharmacodynamic.

figure S10). As shown in figure 6A, incremental doses of IL-15 caused incremental proliferation and expansion of target effector cells, but never to the extent of MS~IL-$15_{50\,\mu g}$. The 25 µg dose of IL-15 is dose-equivalent to the $IL\text{-}15_{AP}$ released from MS~IL-$15_{50\,\mu g}$ over 1 week, and the 50 µg supra-high dose is equivalent to the total amount of IL-15 on MS~IL-$15_{50\,\mu g}$. In all cases, the PD responses of the single doses examined are much lower than the long-acting MS~IL-$15_{50\,\mu g}$.

The magnitude of the PD effect by an IL-15 agonist depends on a sufficient level of target engagement for a sufficient period of time,[10–12] and wasted cytokine excess over receptor saturation increases C_{max} but not signal intensity. As dose is increased, C_{max} increases linearly whereas the time during which receptors are effectively saturated increases logarithmically (online supplemental section XII). Figure 6A, inset, shows that $AUC_{28\,d}$ of proliferation and expansion of immune cells versus IL-15 concentrations fit very well to a logarithmic relationship; in contrast, as illustrated for $CD44^{hi}CD8^+$ T cells, when the response between 0 and 5 µg IL-15 is used to define a linear slope the fit is very poor. Hence, the observed PD effects of single varying doses of IL-15 are not correlated with C_{max}, but rather with the time receptors are occupied with sufficient IL-15 to expand immune cells.

We likewise inquired whether the high immune cell expansion after five daily doses of 5 µg IL-15 occurred abruptly during the study period, or increased steadily with repeated doses. Mice were administered doses of 5 µg IL-15 for 1–5 successive days (online supplemental figure S11). Here, the $AUC_{28\,d}$ of proliferating NK and $CD44^{hi}CD8^+$ T cells were linear (R^2=0.93) with the frequency of doses (figure 6B), as expected if each dose increased the time of exposure over some adequate target concentration. Taken together, the results indicate that optimal time-over-target cannot be achieved by single doses of different IL-15 quantities but can by multiple sequential doses of IL-15 or by a single administration of the long-acting MS~IL-$15_{50\,\mu g}$.

We also examined the PD effects of the super-agonist RLI, a single chain fusion of IL-15, and the 77 aa IL-15Rα sushi connected by a 20-amino acid linker. As an IL-15Rα-independent agonist, RLI binds with ~100-fold higher affinity to the intermediate affinity IL-2Rβ/γc than IL-15[22 34] and has ~6-fold longer $t_{1/2}$ in mice (table 1).[35] As shown in figure 6A, 10 µg of RLI—equimolar to 6 µg IL-15—produces a PD effect >25 µg IL-15, and two doses of only 2 µg RLI separated by 2 days produces expansions superior to 10 µg of RLI or 50 µg IL-15. As with IL-15, the duration of receptor occupancy by RLI appears to play a more important role than dose intensity.

MS~IL-15 with an alternative linker and in vivo release rate

In early experiments, we also prepared and partially characterized an MS~IL-15 with the same $MeSO_2$ modulator as in MS~IL-15 placed on a gem-dimethyl substituted linker[36] designated MS_{GDM}~IL-15. The in vitro release $t_{1/2}$ extrapolated to pH 7.4, 37°C was 1000 hours, close

to that of MS~IL-15. However, in C57BL/6J mice the $t_{1/2}$ of released IL-15_{AP} was 50 hours—still longer than any reported IL-15 agonist—but showed no second phase of CL. As calculated above for MS~IL-$15_{50\,\mu g}$, we estimated the IL-15_{AP} released from MS_{GDM}~IL-$15_{50\,\mu g}$ over day 5 to be an average of ~8 µg/day. When MS_{GDM}~IL-$15_{50\,\mu g}$ was injected in mice, analysis of duration and $AUC_{28\,d}$ of immune cell expansion was very similar, if not identical, to MS~IL-$15_{50\,\mu g}$ (online supplemental figure S12 and table S2); thus, it appears that a $t_{1/2}$ of 50 hr provides sufficient exposure to achieve optimal PD effects. Regardless, the present work focused on studies of MS~IL-15 because the longer $t_{1/2}$ of released IL-15_{AP} over 5 days more resembled that of the target 5-day CIV of IL-15.

Tolerability and safety of MS~IL-15

Toxicity and injection site reactions of subcutaneously administered MS_{GDM}~IL-15 were assessed in mice. A complete summary of the study is provided in SI. Briefly, male C57BL/6J mice (n=6/group) were administered 0.1 mL of blank MS, MS_{GDM}~IL-$15_{150\,\mu g}$, or MS_{GDM}~IL-$15_{500\,\mu g}$ on days 1 and 15 via subcutaneous injections and animals were observed for 28 days. There were no IL-15-related clinical pathologies, organ weight abnormalities, macroscopic findings, bodyweight changes, or dose-dependent microscopic differences between MS_{GDM}~IL-$15_{150\,\mu g}$ and MS_{GDM}~IL-$15_{500\,\mu g}$. Slight injection site swelling and minimal to moderate subcutaneous granulomatous inflammation was observed in all groups and there was a single occurrence of mild myofiber degeneration/regeneration with MS_{GDM}~IL-$15_{150\,\mu g}$. Hence, MS_{GDM}~IL-15 administered day 1 and day 15 containing 150 or 500 µg IL-15/animal/injection—releasing 6-fold to 20-fold more IL-15 than the standard single dose of MS~IL-$15_{50\,\mu g}$ used in this study—was generally well tolerated by mice.

Effect of MS~IL-15 and agonistic anti-CD40 on the TRAMP-C2 prostatic cancer model

In a previous study, a combination of IL-15, systemically administered at 2.5 µg/mouse 5 days/week×2, and anti-CD40 showed high synergistic antitumor activity in the primarily $CD8^+$ T cell-driven murine TRAMP-C2 prostatic cancer model.[24] Figure 7 shows the effects of subcutaneously administered IL-15 (figure 7A) or MS~IL-$15_{50\,\mu g}$ (figure 7B) and IT administered anti-CD40 agonist in a bilateral syngeneic murine TRAMP-C2 model (Chen *et al* 2021, submitted). Here, the right tumor in each animal was injected with anti-CD40, and animals received ten intraperitoneal doses of 2.5 µg IL-15 over 14 days or a single subcutaneous dose of MS~IL-$15_{50\,\mu g}$. The combination of MS~IL-15_{50}

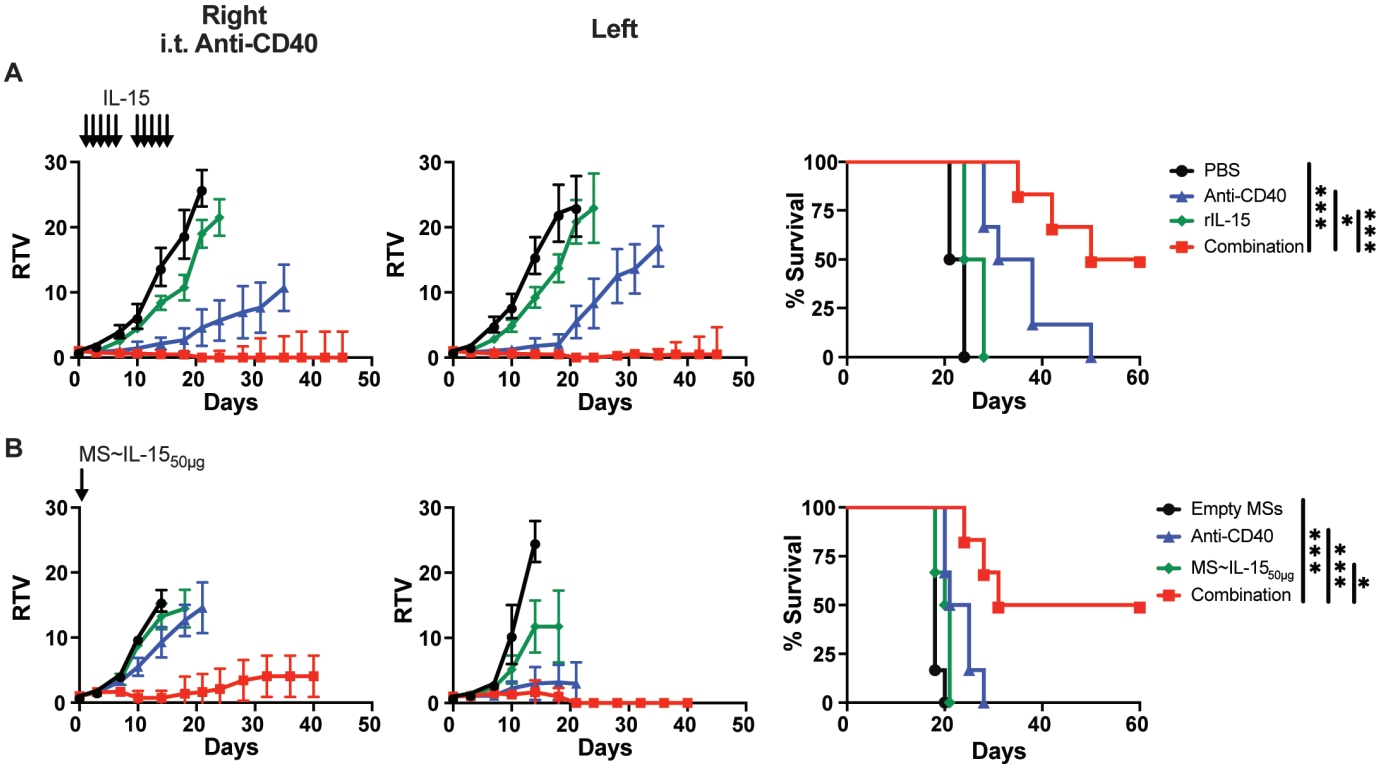

Figure 7 Antitumor effects of IL-15 and MS~IL-15 in the TRAMP-C2 prostate tumor model. (A) RTV of C57BL/6J mice (n=6/group) bearing TRAMP-C2 tumors on both flanks were treated with intraperitoneal 2.5 µg IL-15 (days 1–5, 8–13), IT anti-CD40 mAb (20 µg/10 µL on days 0, 3, 7, and 10) in the right-flank tumor or the combination of IL-15 plus anti-CD40; the Kaplan-Meier plot shows per cent of surviving mice. The control group was injected with PBS. (B) Same as top panel except using a single dose of subcutaneous MS~IL-$15_{50\,\mu g}$ instead of multiple doses of IL-15. The control group was injected subcutaneously with empty MS. Data shown as relative median tumor volume ±SE of the median. Two-way analysis of variance and log-rank (Mantel-Cox) tests were used to determine statistical differences. *P<0.05, ***p<0.001. IL, interleukin; IT, intratumoral; MS, microspheres; mAb, monoclonal antibody; PBS, phosphate-buffered saline; RTV, relative median tumor volume.

μg and anti-CD40 resulted in significant expansion in the absolute number of peripheral $CD8^+$ T cells, $CD44^{hi}CD8^+$ T cells, and tumor-specific $tetramer^+CD8^+$ cells compared with either monotherapy (online supplemental figure S13). Growth of both tumors in mice injected with single agent anti-CD40, IL-15, or MS~IL-$15_{50\ \mu g}$ showed modest tumor growth inhibition. However, growth of tumors in mice receiving both unilateral IT anti-CD40 and systemic IL-15 or MS~IL-$15_{50\ \mu g}$ were suppressed for long periods. As shown in figure 7B, none of the mice in the single agent MS~IL-$15_{50\ \mu g}$ or anti-CD40 groups survived, whereas 50% of the mice in the MS~IL-$15_{50\ \mu g}$/anti-CD40 combination group were alive at day 60, all being tumor free. Hence, the combination of systemic MS~IL-$15_{50\ \mu g}$ and unilateral IT anti-CD40 produce a potent effect on the tumor injected with anti-CD40 as well as the non-injected tumor.

Effect of MS~IL-15 and anti-CCR4 (mogamulizumab) on the MET-1 murine model of ATL)

It has been reported that IL-15 caused a NK cell-driven prolongation of survival of MET-1 tumor-bearing mice and thereby increased efficacy of anticancer mAbs through ADCC.[26] Since the CC-chemokine receptor CCR4 is expressed on the surface of leukemic cells in most ATL cases,[37] the MET-1 ATL model in NOD/SCID mice that lack T and B cells[25] was used to test MS~IL-15 in combination with anti-CCR4. After intraperitoneal injection of MET-1 cells when serum-soluble human IL-2Rα—a surrogate tumor marker[38]—reached 1000 pg/mL, mice were treated with a single dose of MS~IL-$15_{50\ \mu g}$, every week×4 anti-CCR4, or the combination of MS~IL-$15_{50\ \mu g}$ with every week×4 anti-CCR4 (figure 8A). We confirmed the expression of CCR4 and CD25 on the MET-1 leukemia cells (figure 8B). Treatment with MS~IL-$15_{50\ \mu g}$ markedly increased the NKp46 cells in blood compared with the phosphate-buffered saline

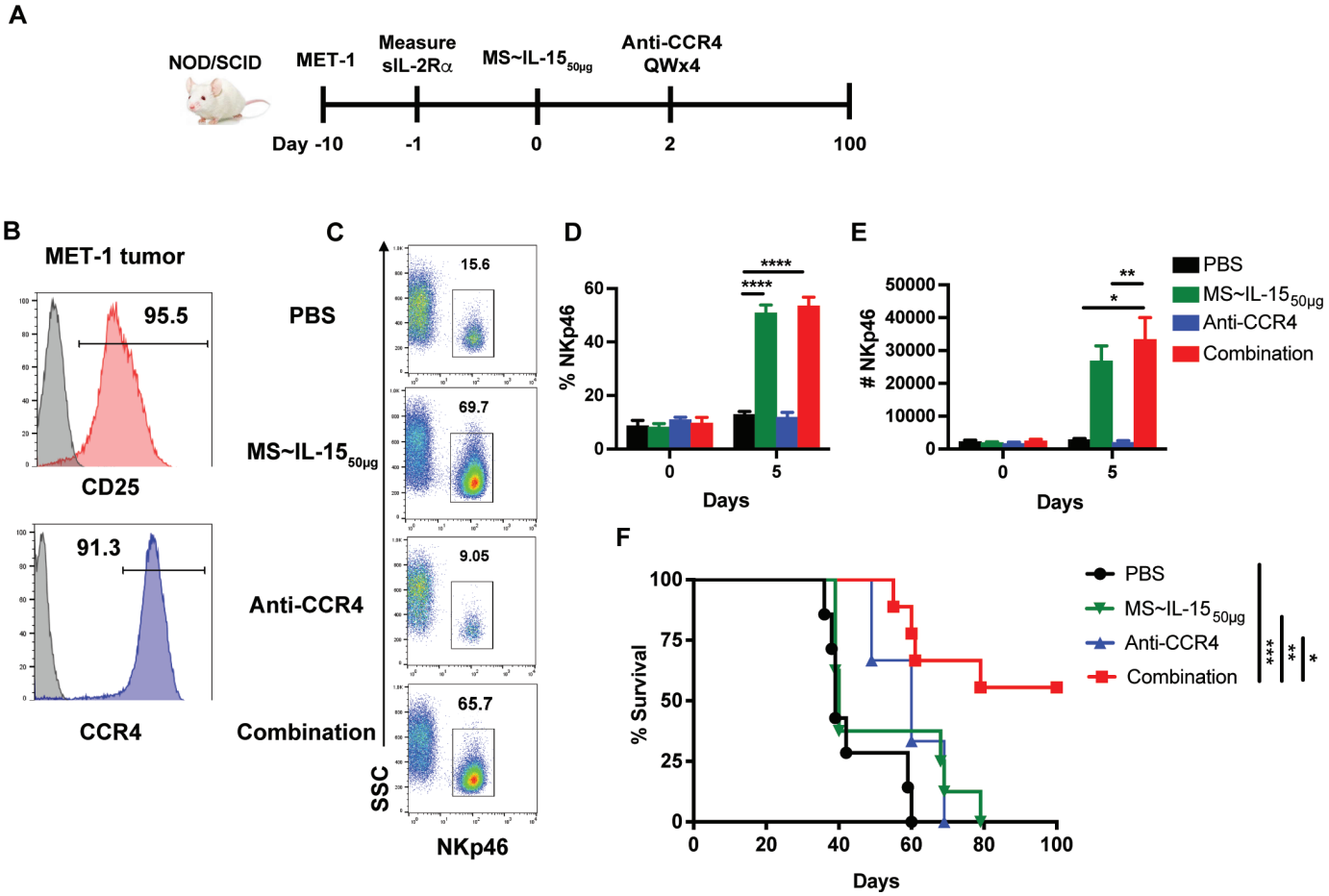

Figure 8 Treatment of MET-1-bearing NOD/SCID mice with MS~IL-$15_{50\ \mu g}$ and anti-CCR4 antibody. (A) Experimental scheme of the xenograft model of human MET-1 leukemia. Ten days after intraperitoneal injection of leukemia cells (2×10^7 MET-1 cells) in NOD/SCID mice (n=3 for anti-CCR4 to 9/group), animals were treated with PBS or subcutaneous MS~IL-$15_{50\ \mu g}$; after 2 days, 100 μg of CCR4 antibody was given intraperitoneally QWk×4. (B) Expression of CD25 and CCR4 on MET-1 tumor. (C) Representative flow cytometric analysis of NKp46 in blood on day 5 after MS~IL-15 injection. (D–E) NKp46 cells in blood on day 5. (F) Kaplan-Meier curves illustrating the survival of mice that received PBS, MS~IL-$15_{50\ \mu g}$, anti-CCR4, or the combination of MS~IL-$15_{50\ \mu g}$ and anti-CCR4. The survival of the mice was recorded until day 100 post-therapy. Two-way analysis of variance and log-rank (Mantel-Cox) tests were used to determine statistical differences. *P<0.05, **p<0.01, ***p<0.001, ****p<0.0001. IL, interleukin; IT, MS, microspheres; NK, natural killer; PBS, phosphate-buffered saline; QWk, every week.

and anti-CCR4 groups (figure 8C–E). At 100-day post-treatments, 50% of the mice receiving combination of MS~IL-15$_{50\ \mu g}$ and anti-CCR4 survived, whereas all others expired (figure 8F). Hence, the combination of MS-IL-15 and anti-CCR4 was highly effective at prolonging the survival of mice-bearing MET-1 leukemia.

DISCUSSION

Since the discovery of IL-15 in 1994,[39 40] extensive efforts have been expended toward its development as an immuno-oncology agent.[2 3] Foremost in achieving this goal have been endeavors to control the effects of IL-15 on NK and CD8$^+$ T cells, which link the cytokine to its therapeutic effects. More recently, the effects of IL-15 on γδ T cells have received much interest because of their dual effects on both innate and adaptive immune responses, and potential importance in cancer immunotherapy.[41 42] Optimal immune cell expansion requires IL-15 exposure at a level above a threshold concentration for a protracted period—a critical time-over-target.[10–12] Since lower concentrations or times are not optimally efficacious, and higher concentrations or times may contribute to toxicities, an appropriate balance of agonist level and duration of exposure is essential. A major impediment to the success of IL-15 as an immunotherapeutic is that it has a short in vivo half-life of only 2.5 hours in the human; the high dose of a single injection necessary to achieve sufficient sustained exposure is accompanied by a high C_{max} and associated toxicities.[13] Hence, extensive efforts have been directed toward developing long-acting IL-15 agonists that remain within a narrow therapeutic window for long periods and achieve an optimal time-over-target.

In one approach, IL-15 super-agonists have been developed that increase potency and extend $t_{1/2}$ by incorporation of IL-15Rα and, in some cases, an Fc fragment—those in current clinical development include N-803, hetIL-15, and RLI.[14] When administered intravenously to humans, these super-agonists have elimination $t_{1/2}$s of ~1.5 to 7.5 hours, which are not significantly different than the 2.5 h $t_{1/2}$ of intravenously administered IL-15. However, when administered subcutaneously, the effective $t_{1/2}$s are modestly increased to 4–24 hours because of slow absorption from their injection sites.[31 43 44] In addition to slow absorption, some of the larger super-agonists are also *poorly* absorbed resulting in very low and potentially problematic bioavailability. For example, subcutaneously administered N-803—a large IL-15Rα-Fc complex with IL-15 N72D—has only 3% bioavailability which indicates that 97% of the agonist is disposed of at the injection site; the high residual IL-15 activity may recruit immune cells that cause the injection site rashes commonly seen with this agonist.[43] Although IL-15 has been attached to other long-lived Fc or IgG fragments, longer-acting agonists have not materialized.[14] In another approach, high MW PEG has been attached to IL-15 to provide NKTR-255 which when administered intravenously to humans gave a $t_{1/2}$ of ~24 hours[45]; this makes NKTR-255 one of the IL-15 agonist front-runners, but the $t_{1/2}$ is far from what is often achievable by PEGylation. In an alternative tactic, IL-2 has been PEGylated—for example, bempegaldesleukin and THOR-707—to bias binding toward IL-2Rβ/γc such that the effects on immune cells mimic those of IL-15[46]; these agonists also have modest $t_{1/2}$ values of ~12 hours. Finally, the most effective approach to maintain optimal levels of IL-15 over time has been to administer IL-15 via 5-day or 10-day CIV, which show remarkable increases of CD8$^+$ T cells, NK cells, and CD56^{bright} NK cells as well as impressive expansion of γδ T cells.[15 16] However, CIV administration is a generally unacceptable and impractical mode of administration.

The primary objective of the present work was to develop a subcutaneously administered long-acting IL-15 that would, insofar as possible, mimic the PK of CIV and expand target immune cells levels over an extended period. We first prepared and characterized hydrogel MS covalently attached to the N-terminus of IL-15 by a β-eliminative linker that slowly releases the agonist. We then studied the PKs of subcutaneously administered MS~IL-15 as well as its effect on expansion of target NK and CD8$^+$ T cells. Lastly, we demonstrated that a single dose of MS~IL-15 is extremely effective in immunotherapy of cancer in both NK and CD8$^+$ T cell-driven murine tumor models. Thus, with MS~IL-15 we have developed a slow releasing depot of IL-15 which after a single subcutaneous injection causes an effective and persistent increase of NK and CD44^{hi}CD8$^+$ T cells and high activity as an immunotherapeutic agent.

To prepare MS~IL-15, we first attached an azido-linker-aldehyde to the N-terminus of IL-15 by reductive amination using a stoichiometry that favors mono-alkylation versus multi-alkylation. Then, we attached the azido-linker-IL-15 to cyclooctyne-activated MS by strain-promoted azide-alkyne cycloaddition. The IL-15 in the MS~IL-15 depots exceeded 95% purity and was stable under physiological and storage conditions for prolonged periods. On β-eliminative cleavage of the linker, IL-15$_{AP}$ is released from the MS~IL-15, which was equipotent to IL-15 in a cell-based IL-2Rβ/γc dimerization assay.

On subcutaneous administration of MS~IL-15 containing 50 µg of IL-15 (MS~IL-15$_{50\ \mu g}$) to mice, the released IL-15$_{AP}$ maintained the ~200 to 300 pM plasma concentration of IL-15 effective in CIV[16 29] with a $t_{1/2}$ of about 1 week for 5 days—far longer than any IL-15 agonist thus far reported.[14] It was serendipitous that the 5-day duration of high exposure of the released agonist was a similar duration as that of the 5-day CIV we sought to emulate.[15] Interestingly, after ~5 days there was an abrupt decrease in $t_{1/2}$ to about ~30 hours, which was maintained for a several week period. The biphasic PKs were not observed in immune-deficient NSG mice and we did not detect anti-IL-15 antibodies that might increase CL. Similar time-dependent increases in CL observed with the super-agonist hetIL-15[31] and CIV infusion of IL-15[16 29] have been attributed to formation of a dynamic IL-15 sink that consumes the cytokine, and the present study supports this hypothesis.

Most reported studies of IL-15 in mice use a paucity of measurements over time to quantitate expansion of immune cells. We measured target immune cell expansion in spleen, lymph nodes, and PBMCs over a 28-day period which—although tedious—covers the complete duration of immune cell expansion observed with MS~IL-$15_{50\ \mu g}$. To quantify proliferation and expansion, we developed an approach that measures the duration and extent that cells remained over controls. Here, we quantified the AUC of cell expansion over the 28-day study period, which is analogous to that commonly used in pharmacology to measure drug exposure over time. This approach allowed us to quantitatively compare long duration PD effects elicited by MS~IL-15 that would be difficult to accomplish by conventional methods. We showed that $AUC_{28\ d}$ correlated well among tissues examined, and that MS~IL-15 elicits very prolonged and very robust PD effects on its target immune cells. Hence, measurements of $AUC_{28\ d}$ provides compelling benefits over other approaches for quantitation of immune cell expansion by long-acting IL-15 agonists.

A single dose of MS~IL-$15_{50\ \mu g}$ resulted in protracted cell expansion of ~14 days for NK, $CD8^+$, and γδ T cells, and a very long 28 days for $CD44^{hi}CD8^+$ T cells. Indeed, the duration and expansion of immune cells elicited by MS~IL-$15_{50\ \mu g}$ far exceeded alternative dose-equivalent administrations of free IL-15. For example, the PD effects of MS~IL-$15_{50\ \mu g}$ greatly surpassed those from a single dose of 25 µg IL-15—the estimated amount of $IL\text{-}15_{AP}$ released from MS~IL-$15_{50\ \mu g}$ over 5 days—as well as 50 µg IL-15—the total amount of IL-15 present on MS~IL-$15_{50\ \mu g}$. Also, the average $AUC_{28\ d}$ values of proliferation and expansion of immune cells by MS~IL-$15_{50\ \mu g}$ exceeded those from five daily injections of 5 µg IL-15 by ~150%. Interestingly, $MS_{GD\text{-}M}$~IL-$15_{50\ \mu g}$ with a monophasic $t_{1/2}$ of 50 hr showed similar PD effects as the longer acting MS~IL-$15_{50\ \mu g}$ and may represent the minimal exposure time of IL-15 to provide an optimal PD effect. Hence, compared with various dose-equivalent schedules of IL-15, MS~IL-15 conjugates provide remarkably long and intense PD effects.

We also determined $AUC_{28\ d}$ of immune cell expansion after injections of varying amounts and frequencies of IL-15 and the super-agonist RLI. The $AUC_{28\ d}$ of immune cell expansion after single doses of varying amounts of IL-15 did not increase linearly as expected if expansion was directly related to dose and C_{max}. Rather, proliferation and expansion of NK and $CD44^{hi}CD8^+$ T cells increased logarithmically with dosage, indicating that increasing doses affected the time over which the cytokine remained at a concentration needed for receptor occupancy and activation. With the super-agonist RLI—which has a higher affinity for IL-2Rβ/γc receptor and longer $t_{1/2}$ than IL-15—two doses of only 2 µg separated by 2 days—equimolar to only 1.2 µg IL-15×2—produced expansions superior to a single dose of 10 µg RLI or 50 µg IL-15. Finally, the dose-linear $AUC_{28\ d}$ of immune cell expansion after sequential single doses of 5 µg IL-15 was also consistent with linearly increasing the time of exposure. Taken together, these data show that the PD effects of different doses of IL-15 are not directly correlated with C_{max}, but rather with the time receptors are occupied with sufficient IL-15 to expand immune cells. Hence, the necessary time-over-target for optimal expansion cannot be achieved by single doses of IL-15 because of its short $t_{1/2}$, but can by multiple sequential doses or by the slow, steady release of IL-15 from a single subcutaneous administration of long-acting MS~IL-$15_{50\ \mu g}$.

These results all support the view that optimal in vivo proliferation of immune cells requires IL-15 exposure at a level above some minimal threshold concentration for some minimal period of time. However, cytokine stimulation that is too sustained or too frequent may be detrimental to immune cell expansion or function,[33 47 48] and the optimal in vivo exposure time or level is yet to be determined. For example, Elpek *et al*[47] found that transient treatment of mice with potent IL-15/IL-15Rα complexes increased the number and effector functions of activated NK cells, whereas prolonged stimulation led to accumulation of mature NK cells with impaired function. Likewise, Frutoso *et al*[33] reported NK cell hyporesponsiveness to IL-15 agonists in mice whereby a second dose administered as long as 50 days after the first resulted in a large attenuation in NK-cell proliferation. On a second treatment of mice with MS~IL-15 1 month after the first, we also observed NK cell hyporesponsiveness. However, there are substantial interspecies differences in NK cell subsets and cell surface receptors in mice and humans, so the IL-15-induced NK hyporesponsiveness in mice need not translate to humans.[49 50] Indeed, in non-human primates and humans immune cell responsiveness and effector functions do not appear significantly impaired after multiple doses of N-803,[43 51] RLI,[44 52] NKTR-255,[45] or by CIV IL-15,[15 16 29] especially if a suitable rest interval is allowed between doses or treatment cycles. In view of the apparent species differences of NK cell hyporesponsiveness and exhaustion, we did not consider it necessary to resolve these issues in mice and did not pursue further studies of multiple doses of MS~IL-15.

Finally, MS~IL-15 was assessed as an immunotherapeutic agent in two murine tumor models. First, it was tested in combination with IT-administered agonistic anti-CD40 in a bilateral TRAMP-C2 model of prostatic cancer (Chen, submitted), primarily driven by cytotoxic $CD8^+$ T cells.[24] A single subcutaneous injection of MS~IL-$15_{50\ \mu g}$ and IT CD40 agonist in one of the tumors showed modest growth inhibition when individually administered, but evoked robust antitumor activity in both tumors when administered as a combination. Second, in the MET-1 model of ATL,[26] driven by NK cells, a single dose of MS~IL-$15_{50\ \mu g}$ caused a very large expansion of NK cells. Single-agent MS~IL-$15_{50\ \mu g}$ or anti-CCR4 provided modest increases in survival, but a combination of both significantly prolonged survival. Clearly, MS~IL-15 should be pursued as an immunotherapeutic agent in human cancers, especially in combination with other agents that may be synergistic with the cytokine.

In summary, the MS~IL-15 prodrug provides a very long-acting IL-15—longer than any known IL-15 agonist—and the PD effects are likewise longer lasting than any IL-15 agonist yet reported. The IL-15 released from the MS has a low C_{max} and causes protracted high expansion of NK cells and γδ and $CD44^{hi}CD8^{+}$ T cells. MS~IL-15 shows robust anticancer activity in NK and cytotoxic $CD8^{+}$ T cell-driven responses, especially when administered in combination with other immunotherapeutic agents. From our perspective, important future work entails studies of MS~IL-15 in non-human primates and then in human clinical trials. Also, further studies on the MS delivery system should address (a) determining the optimal $t_{1/2}$ of IL-15 release from the depot—sufficient but not excessive to produce optimal PD effects, (b) investigating the effects of an MS prodrug of a more potent, longer-acting super-agonist, such as the IL-15Rα-independent agonist RLI, and (c) applying the technology to other cytokines that could benefit from half-life extension. Since the PKs of MS~IL-15 are largely due to the nature of the β-eliminative linker connecting IL-15 to the carrier, and the rate of release is species-independent, we are optimistic that results obtained here will translate from mouse to man.

Acknowledgements The authors would like to dedicate this manuscript to Dr Thomas Waldmann. The authors would like to thank Drs Christopher Carreras, Hongruo Yun, Shaun Fontaine, Jeff Henise, Rocio Fernandez, and Guillermo Hails for technical assistance, Dr Bora Han for advising on the toxicology study, and Dr Gary Ashley for insightful discussions.

Contributors Conceptualization: DVS, TAW. Investigation: JAH, WC, SPD, AD, JRM, RR. Supervision: DVS, TAW. Writing: DVS, TAW, JAH. WC, SPD, and AD contributed equally. Guarantor: DVS.

Funding Some flow cytometry data reported was collected at the UCSF Helen Diller Family Comprehensive Cancer Center Lab for Cell Analysis, which is supported by the National Cancer Institute of the National Institutes of Health under Award Number P30CA082103.

Disclaimer The content is solely the responsibility of the authors and does not necessarily represent the official views of the National Institutes of Health.

Competing interests JAH, RR, and DVS are employees and hold options or stock in ProLynx Inc. All other authors declare that they have no competing interests.

Patient consent for publication Not applicable.

Ethics approval Animal experiments performed at the NIH/NCI were approved by the NCI Animal Care and Use Committee and were performed in accordance with NCI Animal Care and Use Committee guidelines. All other animal handling and care was performed by MuriGenics (Vallejo, California) and Explora Biolabs (San Francisco, California) and conformed to IACUC recommendations.

Provenance and peer review Not commissioned; externally peer reviewed.

Data availability statement All data relevant to the study are included in the article or uploaded as supplementary information.

ORCID iDs
John A Hangasky http://orcid.org/0000-0002-8386-3922
Thomas A Waldmann http://orcid.org/0000-0003-4500-6660

REFERENCES

1 Robinson TO, Schluns KS. The potential and promise of IL-15 in immuno-oncogenic therapies. *Immunol Lett* 2017;190:159–68.
2 Waldmann TA, Miljkovic MD, Conlon KC. Interleukin-15 (dys) regulation of lymphoid homeostasis: Implications for therapy of autoimmunity and cancer. *J Exp Med* 2020;217:e20191062.
3 Waldmann TA, Dubois S, Miljkovic MD, *et al*. IL-15 in the combination immunotherapy of cancer. *Front Immunol* 2020;11:868.
4 Bergamaschi C, Stravokefalou V, Stellas D, *et al*. Heterodimeric IL-15 in cancer immunotherapy. *Cancers* 2021;13:837.
5 Fiore PF, Di Matteo S, Tumino N, *et al*. Interleukin-15 and cancer: some solved and many unsolved questions. *J Immunother Cancer* 2020;8:e001428.
6 Waldmann TA. The biology of interleukin-2 and interleukin-15: implications for cancer therapy and vaccine design. *Nat Rev Immunol* 2006;6:595–601.
7 Dubois S, Mariner J, Waldmann TA, *et al*. IL-15R alpha recycles and presents IL-15 in trans to neighboring cells. *Immunity* 2002;17:537–47.
8 Giron-Michel J, Giuliani M, Fogli M, *et al*. Membrane-bound and soluble IL-15/IL-15Ralpha complexes display differential signaling and functions on human hematopoietic progenitors. *Blood* 2005;106:2302–10.
9 Marks-Konczalik J, Dubois S, Losi JM, *et al*. IL-2-induced activation-induced cell death is inhibited in IL-15 transgenic mice. *Proc Natl Acad Sci U S A* 2000;97:11445–50.
10 Judge AD, Zhang X, Fujii H, *et al*. Interleukin 15 controls both proliferation and survival of a subset of memory-phenotype CD8(+) T cells. *J Exp Med* 2002;196:935–46.
11 Berard M, Brandt K, Bulfone-Paus S, *et al*. IL-15 promotes the survival of naive and memory phenotype CD8+ T cells. *J Immunol* 2003;170:5018–26.
12 Zhao YM, French AR. Mechanistic model of natural killer cell proliferative response to IL-15 receptor stimulation. *PLoS Comput Biol* 2013;9:e1003222.
13 Conlon KC, Lugli E, Welles HC, *et al*. Redistribution, hyperproliferation, activation of natural killer cells and CD8 T cells, and cytokine production during first-in-human clinical trial of recombinant human interleukin-15 in patients with cancer. *J Clin Oncol* 2015;33:74–82.
14 Hangasky JA, Waldmann TA, Santi DV. Interleukin 15 pharmacokinetics and consumption by a dynamic cytokine sink. *Front Immunol* 2020;11:11.
15 Dubois SP, Miljkovic MD, Fleisher TA, *et al*. Short-course IL-15 given as a continuous infusion led to a massive expansion of effective NK cells: implications for combination therapy with antitumor antibodies. *J Immunother Cancer* 2021;9:e002193.
16 Conlon KC, Potter EL, Pittaluga S, *et al*. IL15 by continuous intravenous infusion to adult patients with solid tumors in a phase I trial induced dramatic NK-cell subset expansion. *Clin Cancer Res* 2019;25:4945–54.
17 Santi DV, Schneider EL, Reid R, *et al*. Predictable and tunable half-life extension of therapeutic agents by controlled chemical release from macromolecular conjugates. *Proc Natl Acad Sci U S A* 2012;109:6211–6.
18 Henise J, Hearn BR, Ashley GW, *et al*. Biodegradable tetra-PEG hydrogels as carriers for a releasable drug delivery system. *Bioconjug Chem* 2015;26:270–8.
19 Henise J, Yao B, Ashley GW, *et al*. Autoclave sterilization of tetra-polyethylene glycol hydrogel biomaterials with β-eliminative crosslinks. *Engineering Reports* 2020;2:e12091.
20 Henise J, Yao B, Hearn BR, *et al*. High-throughput, aseptic production of injectable Tetra-PEG hydrogel microspheres for delivery of releasable covalently bound drugs. *Engineering Reports* 2020;2:e12213.
21 Henise J, Fontaine SD, Hearn BR, *et al*. In vitro-in vivo correlation for the degradation of tetra-PEG hydrogel microspheres with tunable β -eliminative crosslink cleavage rates. *Int J Polym Sci* 2019;2019:1–7.
22 Mortier E, Quéméner A, Vusio P, *et al*. Soluble interleukin-15 receptor alpha (IL-15R alpha)-sushi as a selective and potent agonist of IL-15

action through IL-15R beta/gamma. Hyperagonist IL-15 x IL-15R alpha fusion proteins. *J Biol Chem* 2006;281:1612–9.
23 Schneider EL, Hearn BR, Pfaff SJ, *et al*. Approach for half-life extension of small antibody fragments that does not affect tissue uptake. *Bioconjug Chem* 2016;27:2534–9.
24 Zhang M, Ju W, Yao Z, *et al*. Augmented IL-15Rα expression by CD40 activation is critical in synergistic CD8 T cell-mediated antitumor activity of anti-CD40 antibody with IL-15 in TRAMP-C2 tumors in mice. *J Immunol* 2012;188:6156–64.
25 Phillips KE, Herring B, Wilson LA, *et al*. IL-2Ralpha-directed monoclonal antibodies provide effective therapy in a murine model of adult T-cell leukemia by a mechanism other than blockade of IL-2/IL-2Ralpha interaction. *Cancer Res* 2000;60:6977–84.
26 Zhang M, Wen B, Anton OM, *et al*. IL-15 enhanced antibody-dependent cellular cytotoxicity mediated by NK cells and macrophages. *Proc Natl Acad Sci U S A* 2018;115:E10915–24.
27 Nellis DF, Michiel DF, Jiang M-S, *et al*. Characterization of recombinant human IL-15 deamidation and its practical elimination through substitution of asparagine 77. *Pharm Res* 2012;29:722–38.
28 Soman G, Yang X, Jiang H, *et al*. MTS dye based colorimetric CTLL-2 cell proliferation assay for product release and stability monitoring of interleukin-15: assay qualification, standardization and statistical analysis. *J Immunol Methods* 2009;348:83–94.
29 Sneller MC, Kopp WC, Engelke KJ, *et al*. IL-15 administered by continuous infusion to rhesus macaques induces massive expansion of CD8+ T effector memory population in peripheral blood. *Blood* 2011;118:6845–8.
30 Han K-ping, Zhu X, Liu B, *et al*. IL-15:IL-15 receptor alpha superagonist complex: high-level co-expression in recombinant mammalian cells, purification and characterization. *Cytokine* 2011;56:804–10.
31 Bergamaschi C, Watson DC, Valentin A, *et al*. Optimized administration of hetIL-15 expands lymphocytes and minimizes toxicity in rhesus macaques. *Cytokine* 2018;108:213–24.
32 Miyazaki T, Maiti M, Hennessy M, *et al*. NKTR-255, a novel polymer-conjugated rhIL-15 with potent antitumor efficacy. *J Immunother Cancer* 2021;9:e002024.
33 Frutoso M, Morisseau S, Tamzalit F, *et al*. Emergence of NK cell hyporesponsiveness after two IL-15 stimulation cycles. *J Immunol* 2018;201:493–506.
34 Perdreau H, Mortier E, Bouchaud G, *et al*. Different dynamics of IL-15R activation following IL-15 cis- or trans-presentation. *Eur Cytokine Netw* 2010;21:29–307.
35 Bessard A, Solé V, Bouchaud G, *et al*. High antitumor activity of RLI, an interleukin-15 (IL-15)-IL-15 receptor alpha fusion protein, in metastatic melanoma and colorectal cancer. *Mol Cancer Ther* 2009;8:2736–45.
36 Hearn BR, Fontaine SD, Schneider EL, *et al*. Attenuation of the reaction of Michael acceptors with biologically important nucleophiles. *Bioconjug Chem* 2021;32:794–800.
37 Ishida T, Utsunomiya A, Iida S, *et al*. Clinical significance of CCR4 expression in adult T-cell leukemia/lymphoma: its close association with skin involvement and unfavorable outcome. *Clin Cancer Res* 2003;9:3625–34.
38 Tendler CL, Greenberg SJ, Blattner WA, *et al*. Transactivation of interleukin 2 and its receptor induces immune activation in human T-cell lymphotropic virus type I-associated myelopathy: pathogenic implications and a rationale for immunotherapy. *Proc Natl Acad Sci U S A* 1990;87:5218–22.
39 Burton JD, Bamford RN, Peters C, *et al*. A lymphokine, provisionally designated interleukin T and produced by a human adult T-cell leukemia line, stimulates T-cell proliferation and the induction of lymphokine-activated killer cells. *Proc Natl Acad Sci U S A* 1994;91:4935–9.
40 Grabstein KH, Eisenman J, Shanebeck K, *et al*. Cloning of a T cell growth factor that interacts with the beta chain of the interleukin-2 receptor. *Science* 1994;264:965–8.
41 Silva-Santos B, Serre K, Norell H. Gammadelta T cells in cancer. *Nat Rev Immunol* 2015;15:683–91.
42 Vantourout P, Hayday A. Six-of-the-best: unique contributions of γδ T cells to immunology. *Nat Rev Immunol* 2013;13:88–100.
43 Romee R, Cooley S, Berrien-Elliott MM, *et al*. First-in-human phase 1 clinical study of the IL-15 superagonist complex ALT-803 to treat relapse after transplantation. *Blood* 2018;131:2515–27.
44 Podzimkova N, Adkins I, Martynoff Gde, *et al*. 563 Pharmacodynamics and pharmacokinetics of SO-C101 in cynomolgus monkeys. *J Immunother Cancer* 2020;8:A597.
45 Shah N, Tan A, Budde L, *et al*. 355 First-in-human phase I study of NKTR-255 in patients with relapsed/refractory hematologic malignancies. *J Immunother Cancer* 2020;8:A380.
46 Overwijk WW, Tagliaferri MA, Zalevsky J. Engineering IL-2 to give new life to T cell immunotherapy. *Annu Rev Med* 2021;72:281–311.
47 Elpek KG, Rubinstein MP, Bellemare-Pelletier A, *et al*. Mature natural killer cells with phenotypic and functional alterations accumulate upon sustained stimulation with IL-15/IL-15Ralpha complexes. *Proc Natl Acad Sci U S A* 2010;107:21647–52.
48 Felices M, Lenvik AJ, McElmurry R, *et al*. Continuous treatment with IL-15 exhausts human NK cells via a metabolic defect. *JCI Insight* 2018;3:e96219.
49 Guillerey C, Huntington ND, Smyth MJ. Targeting natural killer cells in cancer immunotherapy. *Nat Immunol* 2016;17:1025–36.
50 Zamora AE, Grossenbacher SK, Aguilar EG. Models to study NK cell biology and possible clinical application. *Curr Protoc Immunol* 2015;110:14.37.1–14.
51 Webb GM, Molden J, Busman-Sahay K, *et al*. The human IL-15 superagonist N-803 promotes migration of virus-specific CD8+ T and NK cells to B cell follicles but does not reverse latency in ART-suppressed, SHIV-infected macaques. *PLoS Pathog* 2020;16:e1008339.
52 Marabelle A, Champiat S, Garralda E, *et al*. 807 A multicenter open-label phase I/Ib study of SO-C101 as monotherapy and in combination with pembrolizumab in patients with selected advanced/metastatic solid tumors. *J Immunother Cancer* 2020;8:A856.
53 Chertova E, Bergamaschi C, Chertov O, *et al*. Characterization and favorable in vivo properties of heterodimeric soluble IL-15·IL-15Ralpha cytokine compared to IL-15 monomer. *J Biol Chem* 2013;288:18093–103.
54 Liu B, Jones M, Kong L, *et al*. Evaluation of the biological activities of the IL-15 superagonist complex, ALT-803, following intravenous versus subcutaneous administration in murine models. *Cytokine* 2018;107:105–12.

Supporting Information

A very long-acting IL-15: Implications for the immunotherapy of cancer

John A. Hangasky[1], Wei Chen[2,†], Sigrid Dubois[2,†], Anusara Daenthanasanmak[2,†], Jürgen Müller[2], Ralph Reid[1], Thomas A. Waldmann[2*] and Daniel V. Santi[1*]

[1] ProLynx, San Francisco, CA, United States,
[2] Lymphoid Malignancies Branch, Center for Cancer Research, NCI, NIH, Bethesda, MD, United States

* Contributed equally
† Contributed equally

*Correspondence:
Thomas A. Waldmann, tawald@helix.nih.gov
Daniel V. Santi, daniel.v.santi@prolynxllc.com

Table of Contents

Figures and Tables

I. General Materials and Methods

Materials. Recombinant human IL-15 (>95% pure) was prepared as reported (*1*) and provided by the National Cancer Institute. RLI was produced at ATUM (Newark, CA) based on previously reported methods (*2, 3*). Mogamulizumab-kpkc (NDC code 42747-761-01) was obtained from the NIH Pharmacy. Anti-CD40 (#BP0016-2) was obtained from BioXCell (Lebanon, NH). C57B/6J plasma was purchased from Innovative Research (Novi, MI). All other chemicals and reagents were purchased from commercial vendors unless otherwise stated.

II. Analytical procedures for IL-15

HPLC analysis. HPLC analyses were performed on a Shimadzu LC-20AD HPLC system equipped with a Phenomenex Jupiter 5 µM C18 column (300 Å, 150 x 4.6 mm) heated to 40°C and a SPD-M20A photodiode-array detector. The elution program consisted of a 10-min linear gradient from 20- to 100% CH_3CN containing 0.1% TFA with a flow rate of 1 mL/min.

Mass spectrometry. Proteins were analyzed using LC/ESI-MS on a Waters Acquity UPLC connected to a Waters Xevo QToF mass spectrometer. The LC used a reversed-phase Acquity C4 column at 40ºC. Solvent A was 99.9% H_2O/0.1% HCO_2H and solvent B was 99.9% CH_3CN/0.1% HCO_2H(v/v); the elution program consisted of a linear gradient from 20- to 100%B over 1 minute using a flow rate of 400 µL/min.

Cell-based assays. A U2OS cell-based assay kit for IL-2Rβγ binding was performed according to the manufacturer's instructions (DiscoverX, Part #93-0998E3CP5). Briefly, cells were plated (100 µL, ~5,000 cells/well) in 96 well assay plates and grown for 48 hours at 37ºC, 5% CO_2. Cells were then treated with varying concentrations of the cytokine and incubated for an additional 6 hours at 37ºC, 5% CO_2. Treated cells were then incubated with a chemiluminescent substrate for 1 hour at ambient temperature in the dark prior to luminescence determination with a Spectramax i3 plate reader using a 250 ms integration time.

A CTLL-2 proliferation assay was performed as previously described (*4, 5*). Briefly, cells were cultured in RPMI-1640 medium (ATCC) supplemented with 2 mM L-glutamine, 1 mM sodium pyruvate, 10% fetal bovine serum, and 10% T-STIM with Con A. Prior to assaying, cells were washed three times with RPMI-1640 media containing 10% fetal bovine serum. A 96 well plate was seeded (50,000 cells/well; 100 µL) and incubated for 4 hours at 37ºC, 5% CO_2. A dilution plate containing the rhIL-15 samples in RPMI-1640 media containing 10% FBS was prepared by

10-fold serial dilutions to 2 ng/mL followed by 2 fold serial dilutions to 7.8 pg/mL. Diluted rhIL-15 samples (100 µL) were added to each well and incubated at 37ºC, 5% CO_2. Following a 48 hour incubation, CellTiter96 Aqueous One Solution was added (40 µL) and was incubated for three hours at 37ºC, 5% CO_2. The plate was then read at 490 nm using a Spectramax i3 plate reader.

ELISA. The rhIL-15 concentrations in serum were assessed using a hIL-15 specific ELISA (R&D Systems, hIL-15 Quantikine) performed according to the manufacturer's instructions. Plasma samples were thawed on ice prior to 10- or 50-fold dilution in the standard diluent. *h*IL-15 concentrations were plot as a function of time and fit using GraphPad Prism software.

Flow cytometry. PBMCs were prepared using ACK lysis buffer and incubated with a fixable viability dye to label dead cells. The FcRγII/II receptor was then blocked using CD16/32(2.4G2) (BD). PBMCs were surface stained using optimal Ab concentrations and then fixed for intracellular staining followed protocols from the eBioscience Foxp3/Transcription Factor Staining Buffer Set (ThermoFisher) (Table S1). Stained single cell suspension were analyzed on either FACScan (BD Biosciences) or Attune NxT flow cytometer (Thermofisher). FlowJo cytometry analysis software (TreeStar Inc, Ashland, OR) was used for data analysis. The absolute cell number was determined from complete blood count or by direct cell analysis (Attune NxT).

Table S1. Antibodies used for immunophenotyping.

Antibody	Clone	Vendor
αCD3e-FITC	145-2C11, 17A2	Invitrogen
αCD8a-PercP-Cy5.5	53-6.7	Invitrogen
αCD4-eFluor780	GK1.5	Invitrogen
αNK1.1-PE-Cy7	PK136	Invitrogen
αNK1.1-SuperBright600	PK136	Invitrogen
αCD44-APC	IM7	Invitrogen
αCD44-PE	IM7	Invitrogen
αKi67-APC	SolA15	Invitrogen
αCD19-APC-eFluor780	6D5	Biolegend
αCD19-eFluor450	1D3	Invitrogen
APC-eFluor780 Viability Dye	---	Biolegend
Live/Dead Fixable Aqua dead cell stain	---	Invitrogen
αCD335-PE	29A1.4	Biolegend
αhumanCD194-APC	L291H4	Biolegend
αhumanCD25-FITC	CD25-4E3	Invitrogen
TCRγ/δ-APC	ebioGL3	eBioscience

III. Preparation of MS~IL-15 conjugates

Optimization of azido-linker-IL-15 yield. In a total volume of 75 µL, reactions used 2.25 nmol (0.029 mg, 30 µM) IL-15 in 25 mM Citrate, pH 6.0, 500 mM NaCl and 0.05% tween-20 (Buffer A), 1.5- to 5 equivalents of N_3-PEG_4-L($MeSO_2$)-CHO (2 µg to 7 µg, 45 µM to 150 µM) and 750 nmol (47 µg,10 mM) $NaCNBH_3$. After 20 hours at room temperature, mixtures were treated with 0.5 mM DBCO-PEG_{5kDa} for 4 hours, and analyzed by SDS-PAGE. Here, DBCO-PEG_{5k} reacts with the azide of linker-IL-15 by SPAAC and slows migration (**Fig. S1**) (*6*).

A.

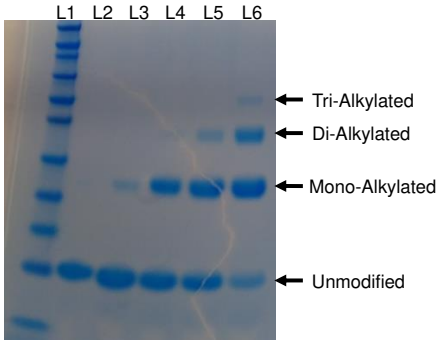

B.

Linker Eq.	% IL-15 Modification			
	Unmodified	Mono-Alkylated	Di-Alkylated	Tri-Alkylated
1.5	54	46	0	0
3	43	52	5	0
5	16	58	22	5

Figure S1. Reductive alkylation of IL-15. A) The progress of reactions were determined by SimplyBlue Safe-stained SDS-PAGE after SPAAC reaction of reductive alkylation mixtures (IL-15_{RM}) with DBCO-PEG_{5kDa}. SDS-PAGE of IL-15_{RM} performed with varying amounts of N_3-PEG_4-L($MeSO_2$)-CHO showing free-, mono- and multi-alkylated IL-15. IL-15 control or IL-15_{RM} (0.5 nmol) were treated with DBCO-PEG_{5kDa} (10 nmol) for 4 hours, then applied to the gel: L1, Novex Sharp Pre-Stained Protein Ladder; L2, IL-15 control; L3, IL-15 + PEG_{5KDa}; L4, N_3-linker:IL-15_{RM} = 1.0; L5, N_3-linker:IL-15_{RM} = 3.0; L6, N_3-linker:IL-15_{RM} = 5.0. B) Percent N_3-linker-IL-15 quantified from data in Panel A using ImageJ software. With 3 equivalents of N_3-linker, the reaction gave 52% IL-15 with 1 linker attached and 5% with two linkers attached. Increasing the N_3-linker to 5 equivalents gave a small increase in mono-alkylated IL-15, but 27% of the IL-15 had ≥two linkers attached.

Preparation of azido-linker-IL-15. In 64 mL of Buffer A, reaction mixtures contained 1.9 µmol (25 mg, 30 µM) IL-15, 5.8 µmol (3.3 mg, 90 µM) of N_3-PEG_4-L($MeSO_2$)-CHO and 640 µmol $NaCNBH_3$ (40 mg, 10 mM). The reaction was allowed to proceed 20 hours at ambient temperature in the dark, at which time the gel-shift assay indicated ~43% unreacted-, 52% monoalkylated- and 5% dialkylated-IL-15. The reaction mixture was concentrated to ~2 mL using an Amicon Ultra 3,500 MW cut-off concentrator and excess reagents were removed using a 14.5 x 50 mm PD-10 column (GE Healthcare) previously equilibrated in Buffer A. The reaction mixture was concentrated to ~1 mL using an Amicon Ultra 3,500 MW cut-off concentrator and the protein concentration (24 mg,

96% recovery) was determined by A_{280} (ε_{280}= 7240 M^{-1} cm^1) using a NanoDrop spectrophotometer.

In a similar fashion and with a similar yield, we prepared azido linker (L=GDM $MeSO_2$) IL-15 using N_3-PEG_4-L(GDM $MeSO_2$)-CHO.

Preparation of MS~IL-15. A slurry of 1.4 mL of BCN-derivatized MSs containing 2.7 µmol BCN/mL in a 10 mL sterile syringe was washed with 5 x 7 mL of Buffer A. The azido-linker-IL-15 reaction mixture containing 1 µmol (~13 mg) of ~50% mono-alkylated IL-15 in 2 mL Buffer A was added to the syringe through a 0.22 µm sterile filter. The mixture was rotated end-over end at ambient temperature for 42 hours, and washed with 6 x 7 mL of Buffer A to remove free IL-15. The unreacted BCN groups were capped by treatment with 1 mL of 50 µmol/mL N_3-PEG_7 (Sigma Aldrich) for 24 hours and the MSs washed with 6 x 7 mL of Buffer A containing 30 mM methionine. MSs were equilibrated with Buffer A containing 30 mM methionine as an anti-oxidant and stored at 4°C. Protein content of the microspheres was determined by A_{280} in 5 mg aliquots of slurry after dissolution in 50 µL of 50 mM NaOH (IL-15; ε_{280}= 7240 M^{-1} cm^{-1}). The PEG content of the conjugate was determined following dissolution through $BaCl_2/I_2$ spectrophotometry. In the present case, in the 2.9 mL of packed gel product there was 975 nmol IL-15 indicating that 97% of the 1 µmol of N_3-linker-IL-15 reactant coupled to the MS-BCN. The PEG content was determined to be 7.9 mg/mL resulting in an IL-15/PEG ratio of 44 nmol IL-15/ mg PEG.

Similarly, we prepared MS_{GDM}~IL-15 by conjugating monoalkylated azido linker (GDM $MeSO_2$) IL-15 (40 mg) to BCN-derivatized MSs (4 µmol) with 80% yield. The concentration of the 1.6 mL of packed MSs was 19.7 mg/mL. The PEG content was determined to be 12.5 mg/mL and the IL-15/PEG ratio was 125 nmol IL-15/mg PEG.

IV. Characterization of MS~IL-15

In vitro release kinetics of MS~IL-15. The release kinetics of MS~IL-15 were determined under accelerated release conditions. Each of ~8 microcentrifuge tubes containing ~10 µL of the MS-IL-15 slurry were diluted with ~40 µL 100 mM NaBorate, 0.05% (v/v) tween-20, pH 9.4, and kept at 37°C. At intervals, samples were centrifuged at 15,000 x g for 2 min and A_{280} of the supernatants were measured using a NanoDrop spectrophotometer. The release rate was calculated by fitting the released A_{280} vs time to a first-order rate equation in GraphPad Prism 8.0, and the $t_{1/2}$ of the hydroxide catalyzed cleavage at pH 7.4 was calculated using the equation:

$$t_{1/2,\ pH\ 7.4} = t_{1/2,\ pH} \times 10^{(pH-7.4)}$$

Purity of IL-15 on MS-IL-15. Purity of the IL-15 conjugated to the microsphere was determined by monitoring the released proteins at pH 9.4, 37ºC, by HPLC. Here, 80 µL of a 350 µM solution was diluted 5-fold in 100 mM NaBorate, 0.05% (v/v) tween-20 pH 9.4, and was distributed into eight 1 mL centrifuge tubes and kept at 37ºC. At intervals spanning over 24 hrs, (~1 half-life of release) samples were centrifuged and 20 µL of the supernatants were analyzed by HPLC. The fraction of each released protein was determined as peak area/total peak areas, and log(peak area) of each component vs time were plotted. The y-intercept of the plot reveals the fraction of each protein present on the MSs at t=0, and the slope of the log IL-15 area vs t plot provides the rate at which IL-15 is degraded in the pH 9.4, 37ºC, buffer.

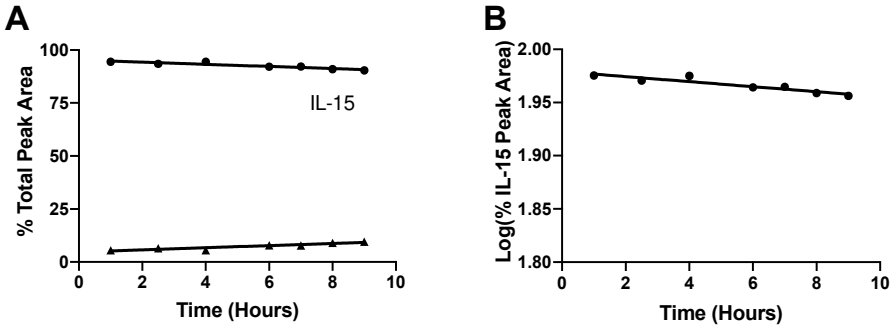

Figure S2. Purity of MS~IL-15. A) Purity of IL-15 bound to the microspheres. B) Rate of degradation of IL-15 at pH 9.4 37ºC. The MS~IL-15 slurry was washed two times and diluted in 125 mM sodium borate pH 9.4, and incubated at 37°C. Released proteins from the microspheres monitored by HPLC. The analysis shows >95% of the protein on the MSs is IL-15. IL-15 degrades in pH 9.4 buffer with a rate of 0.0024 hr^{-1}.

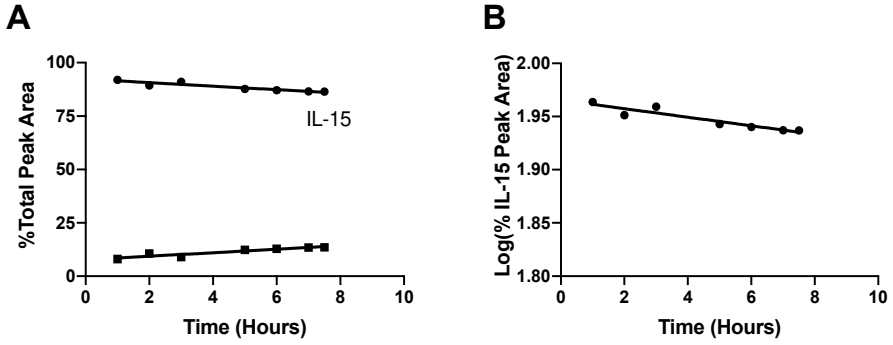

Figure S2B. Assessment of MS~IL-15: 1 month storage stability. A) Purity of IL-15 bound to the microspheres. B) Rate of degradation of IL-15 at pH 9.4 37ºC. The MS~IL-15 slurry was washed two times and diluted in 125 mM sodium borate pH 9.4, and incubated at 37°C. Released proteins from the microspheres monitored by HPLC. The analysis shows following 1 month of storage, >92% of the protein on the MSs is IL-15. IL-15 degrades in pH 9.4 buffer with a rate of 0.0040 hr^{-1}.

Bioactivity of IL-15$_{AP}$. To obtained IL-15$_{AP}$, 75 µL of the MS~IL-15 conjugate was washed 1x with PBS pH 7.4 and then diluted 10 fold in the same buffer. The reaction mixture was incubated at 37ºC for 10 days. The supernatant of the reaction mixture, containing IL-15$_{AP}$, was concentrated to 0.12 mg/mL (10 µM) using an Amicon Ultra 3,500 MW cut-off concentrator. The in vitro activity of IL-15$_{AP}$ was assessed using the U2OS cell-based assay kit for IL-2Rβγ binding.

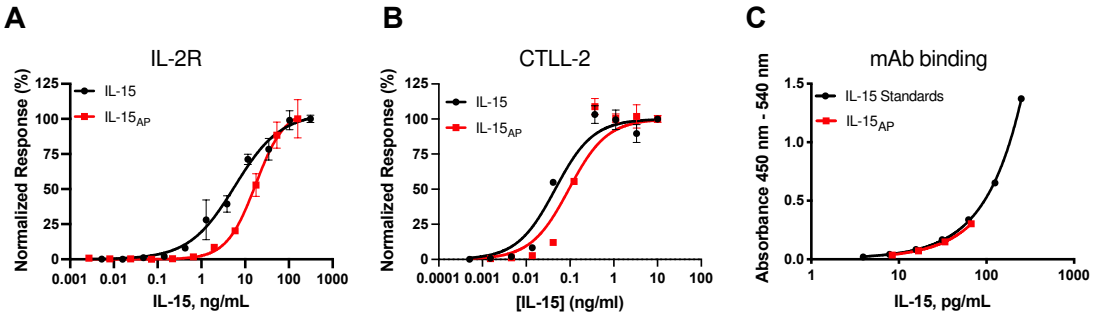

Figure S3. Bioactivity of IL-15$_{AP}$. WT IL-15 (●) and IL-15$_{AP}$ (■) were assayed for A) IL-2Rβγ binding via an U2OS cell-based assay and B) CTLL-2 cell proliferation. Data were fit to a four-parameter logistic model; points are averages ± SD. The EC$_{50}$ for IL-15 induced dimerization of IL-2Rβγ by IL-15 and IL-15$_{AP}$ was determined to be 5.8 ng/mL and 17 ng/mL, respectively. The EC$_{50}$ for IL-15 and IL-15$_{AP}$ CTLL-2 cell proliferation was 46 pg/mL and 94 pg/mL, respectively. C) Antibody binding of IL-15$_{AP}$ assessed via ELISA.

V. Stability studies of free IL-15

The *in vitro* stability of free IL-15 was assessed at pH 7.4, 37ºC and pH 6.0, 4ºC. IL-15 was buffer exchanged into either PBS pH 7.4 or 25 mM Na citrate, 500 mM NaCl, 0.05 tween-20 pH 6.0 using a MidiTrap G-25 desalting column and concentrated to a final concentration of 30 µM (0.385 mg/mL, 1 mL). The sample was divided into two aliquots (2x500µL), with one aliquot spiked with DNP-lysine (10 µM). Samples were incubated at either 37ºC for 10 days or at 4ºC for 28 days. Aliquots (40 µL) were removed over a predefined time course and stored at -80ºC until analysis by a cell-based IL-2Rβγ dimerization assay. DNP-lysine containing samples were analyzed using HPLC over the same time course.

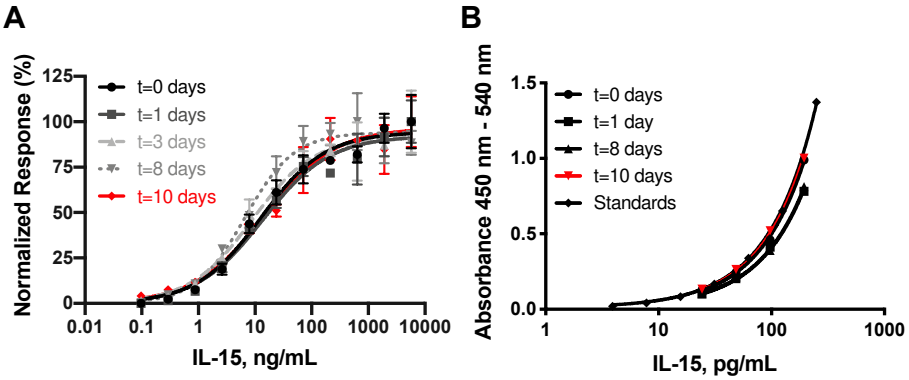

Figure S4. IL-15 bioactivity over 10 days stored at 37°C, pH 7.4. A) The bioactivity of IL-15 was measured by its ability to induce IL-2Rβγ receptor dimerization. Aliquots were taken from a master reaction mixture weekly and frozen at –80°C until all time points were collected. Data were fit to a four-parameter logistic model; points are averages ± SD. The EC_{50} for IL-15 induced dimerization of IL-2Rβγ was determined to 13 ng/mL for the t=0 day time point and 15 ng/mL for the t=10 day time point. B) Antibody binding of $IL\text{-}15_{AP}$ assessed via ELISA.

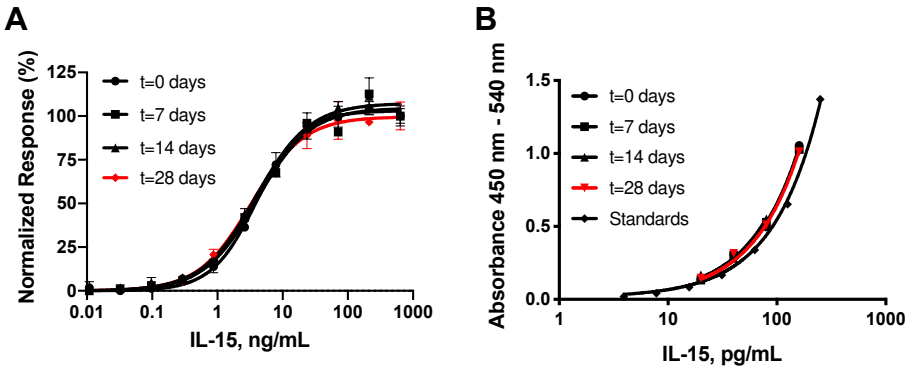

Figure S5. IL-15 bioactivity over 28 days stored at 4°C, pH 6.0**.** A) The bioactivity of IL-15 was measured by its ability to induce IL-2Rβγ receptor dimerization. Aliquots were taken from a master reaction mixture weekly and frozen at –80°C until all time points were collected. Data were fit to a four-parameter logistic model; points are averages ± SD. For all samples, the EC_{50} for IL-15 induced dimerization of IL-2Rβγ was determined to be between 3.3 and 4.0 ng/mL. B) Antibody binding of $IL\text{-}15_{AP}$ assessed via ELISA.

VI. Pharmacokinetic experiments

Preparation of dosing solutions. Dosing solutions were prepared by diluting the MS~IL-15 slurry (275 nmol/mL) in 25 mM Na citrate buffer pH 6.0 containing 500 mM NaCl, 0.05% tween-20 and 1.25% (w/v) hyaluronic acid. To confirm the IL-15 concentration, aliquots of the MS~IL-15 dosing solution(~20 µL) were diluted 5 fold in 50 mM NaOH and incubated for 1 hour at room temperature. Following dissolution of the microsphere conjugate, the reaction mixture (20 µL) was analyzed using standard HPLC methods. A standard curve was prepared using NCI IL-15

standards. IL-15 standards (0.25 mg/mL – 0.004 mg/mL) were prepared from 2-fold serial dilutions in 50 mM NaOH and incubated for 1 hour at room temperature. The concentration of IL-15 in each dosing solution was determined by peak area interpolation of the standard curve.

Pharmacokinetics of MS~IL-15 in immunocompetent mice. Syringes with fixed needles (27 G) were backfilled with the MS~IL-15 conjugate (100 µL). For studies that required various doses of MS~IL-15, serial dilutions were used to obtain the desired MS~IL-15 concentration. The contents of the syringes were administered either SC or IP to normal, male C57BL/6J mice. Blood samples were collected in EDTA collection tubes at -48, 4, 8, 24, 48, 96, 120, 168 and 240 hours from alternating groups of mice (n=3/group). Mice that received a second dose of MS~IL-15 were administered the second injection (100 µL, 50 µg IL15) at 240 hrs. Additional blood draws were taken at 248, 264, 288, 336, 360 and 408 hours. HALT protease inhibitor cocktail was added to all samples and the plasma frozen at –80°C until analysis by ELISA.

Pharmacokinetics of MS~IL-15 in immunodeficient mice. Male, NSG mice (n=3), 6-8 weeks in age, were injected sc with 100 µL of MS~IL-15 (50 µg IL-15) on day 0. Blood samples were collected in EDTA collection tubes containing HALT protease inhibitor at 24 h, 96 h, 168h, 240 h, 336 h, 408h, 504 h, and 576 h post injection. Plasma was prepared and stored at –80°C until analysis by ELISA.

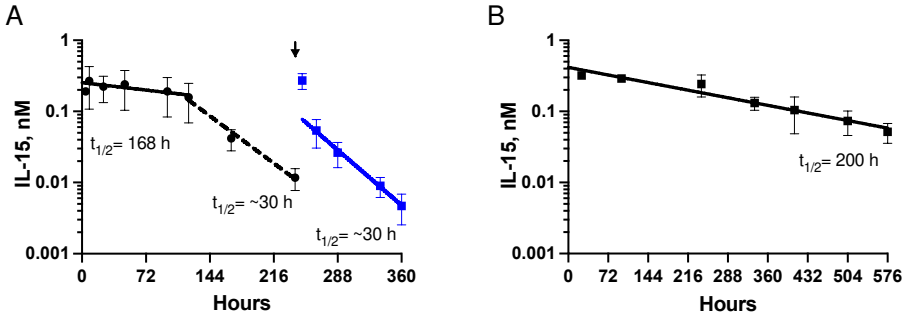

Figure S6. MS~IL-15 pharmacokinetics in immunocompetent and immunodeficient mice. A) C57BL/6J mice were administered SC MS~IL-$15_{50µg}$ on D0 and D10. The black arrow indicates the time of the second administration of MS~IL-15. B) NSG mice (n=6/group) were administered SC MS~IL-$15_{50µg}$ on D0. Plasma was analyzed using R&D System hIL-15 Quantikine ELISA.

VII. Anti-drug antibody ELISA

The presence of anti-rhIL-15 antibodies was assayed for following previously published methods with the following noted exceptions (*1*) . The standard curve for anti-human IL-15 (AF315, R&D Systems) was determined in the presence and absence of 125 pg/mL (10 pM) and 4,000 pg/mL (310 pM) exogenous rhIL-15. Test samples were diluted 9 fold in PBS/1% BSA. Controls were prepared in C57B/6J plasma diluted 9 fold in PBS/1% BSA. All samples and controls were incubated overnight at 4°C. After the assay was developed with p-nitrophenol phosphate (1mg/mL, 100 µL) for 1 hour at 37°C, the absorbance at 405 nm was recorded using a Spectramax i3 plate reader. The limit of detection for an undiluted sample was 195 ng/mL.

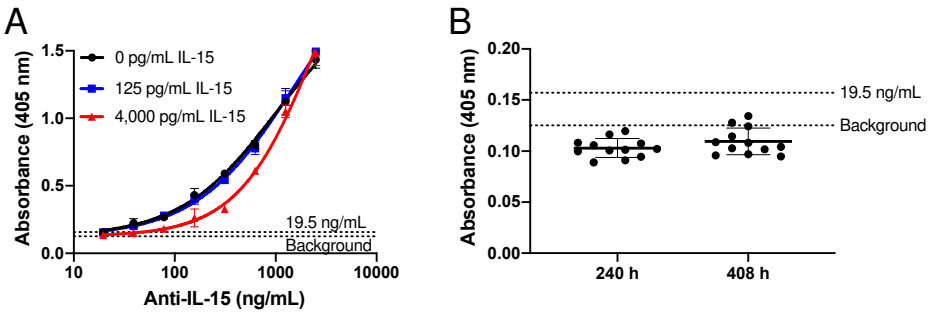

Figure S7. Anti-rhIL-15 antibodies are not detected in mouse plasma. A) Calibration curve for anti-IL-15 antibodies. B) Analysis of test samples for anti-rhIL-15 antibodies (n=12). An affinity purified goat anti-human IL15 (AF315, R&D Systems) was used to define the standard curve in the presence and absence of 125 pg/mL (10 pM) or 4,000 pg/mL (310 pM) exogenous rhIL-15.

VIII. Pharmacodynamics experiments

Pharmacodynamics of MS~IL15 in Spleen, lymph nodes and PBMCs. Normal, male C57black mice (n=18/group) received either a single injection of MS~IL-$15_{50\mu g}$ sc or five daily injection of rhIL-15 (5 µg, QDx5) IP. On days 2, 5, 7, 14, 21 and 28, 3 mice were sacrificed from each group. The spleen and lymph nodes (Superficial cervical, deep cervical, mediastinal, axillary, brachial, mesenteric and inguinal) were harvested and single cell suspensions were prepared. Blood, splenocytes and lymph node lymphocytes were immunophenotyped to quantitate NK cells, B cells, $CD4^+$, $CD8^+$, $CD44^{hi}CD8^+$ and γδ T cells, as well as their proliferating subsets. Prior to the start of the study, five untreated mice were sacrificed to determine baseline cell numbers in the spleen, lymph node and blood. The total AUC for each cell phenotype was determined using Prism. Then, the baseline cell count x 28 was subtracted to yield the AUC_{28d}.

Dose comparison of single or multiple doses of IL-15 to MS~IL-15. A single dose of 5 µg, 10 µg, 25 µg or 50 µg rhIL-15, multiple daily doses of IL-15 (5 µg), a single dose of 10 µg RLI, or two doses of 2 µg RLI (D0 or D2) were administered ip (100 µL) to normal, male C57Black mice (n=4-5/group). An additional group of mice (n=10) received 50 µg MS~IL-15 (Mod: std $MeSO_2$) administered sc (100 µL). Blood samples were drawn on day -2, 2, 5, 7, 14, 21 and 28 and immunophenotyped with an Attune NxT flow cytometer to quantitate B cells, NK cells, CD3, CD4, CD8, and CD44 expressing cells. The total AUC for each cell phenotype was determined using Prism. Then, the baseline cell count x 28 was subtracted to yield the AUC_{28d}.

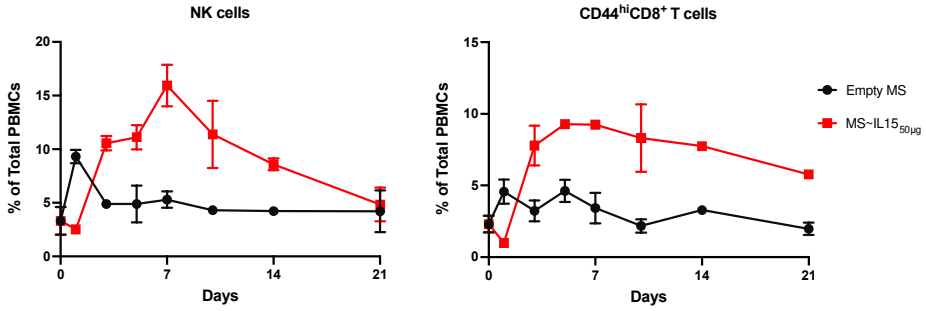

Figure S8. Immune cell response of MS~IL-$15_{50µg}$ compared to empty microspheres. The percentage of NK cells and $CD44^{hi}CD8^{+}$ T cells in PBMCs were measure over 21 days. Mice were administered a single SC dose of MS~IL-$15_{50µg}$ or empty MS (n=3/group).

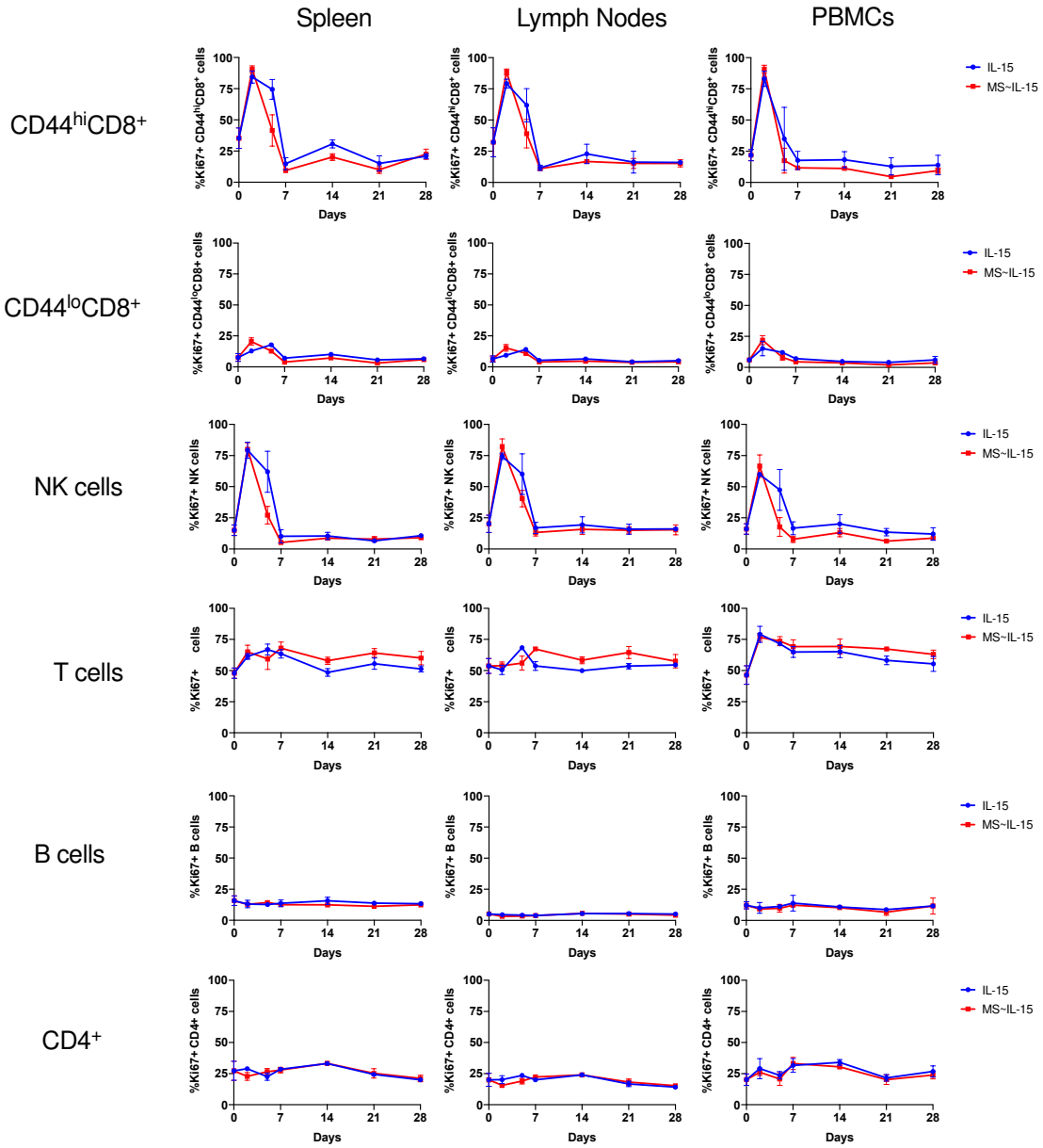

Figure S9A. Proliferation of target immune cells by MS~IL-$15_{50\mu g}$ and 5 µg IL-15 QD x 5 measured over 28 d. Enumeration of NK, $CD8^+$, $CD44^{hi}CD8^+$ T and γδ T cells in the spleen, lymph nodes and blood of mice treated with 50 µg MS~IL-15 (■) or 5 µg IL-15 QD x 5 (●).Tissues were collected (n=3 mice/time point) at 0, 2, 5, 7,14, 21 and 28 d and analyzed for specified cells.

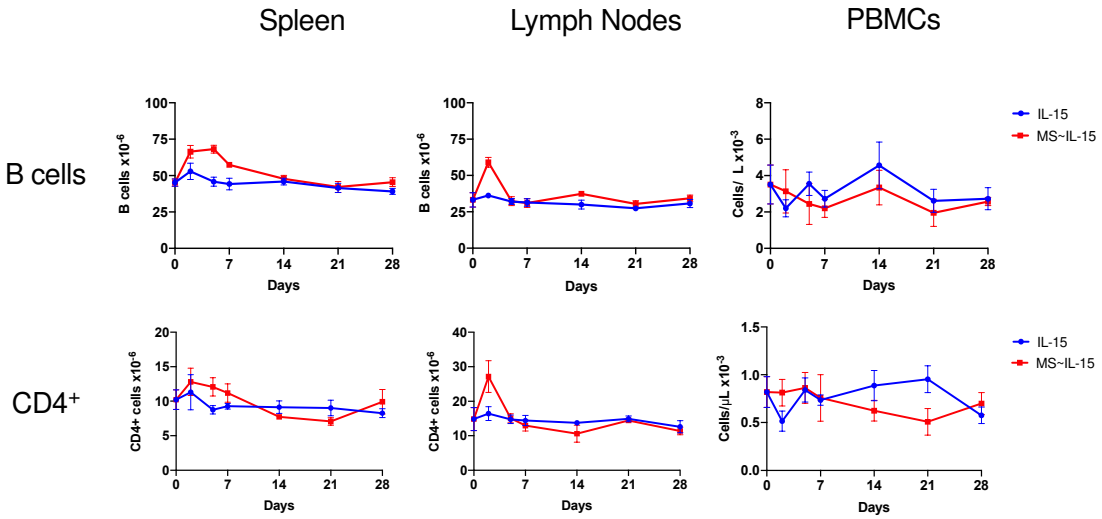

Figure S9B. Immune cell expansion by MS~IL-15$_{50µg}$ over 28 d. Enumeration of CD4$^+$ and B cells at 0, 2, 5, 7,14, 21 and 28 d in the spleen, lymph nodes and PBMCs of mice (n=3/point/group) treated with SC MS~IL-15$_{50µg}$ (■) or IP 5 µg IL-15 QD x 5 (●).

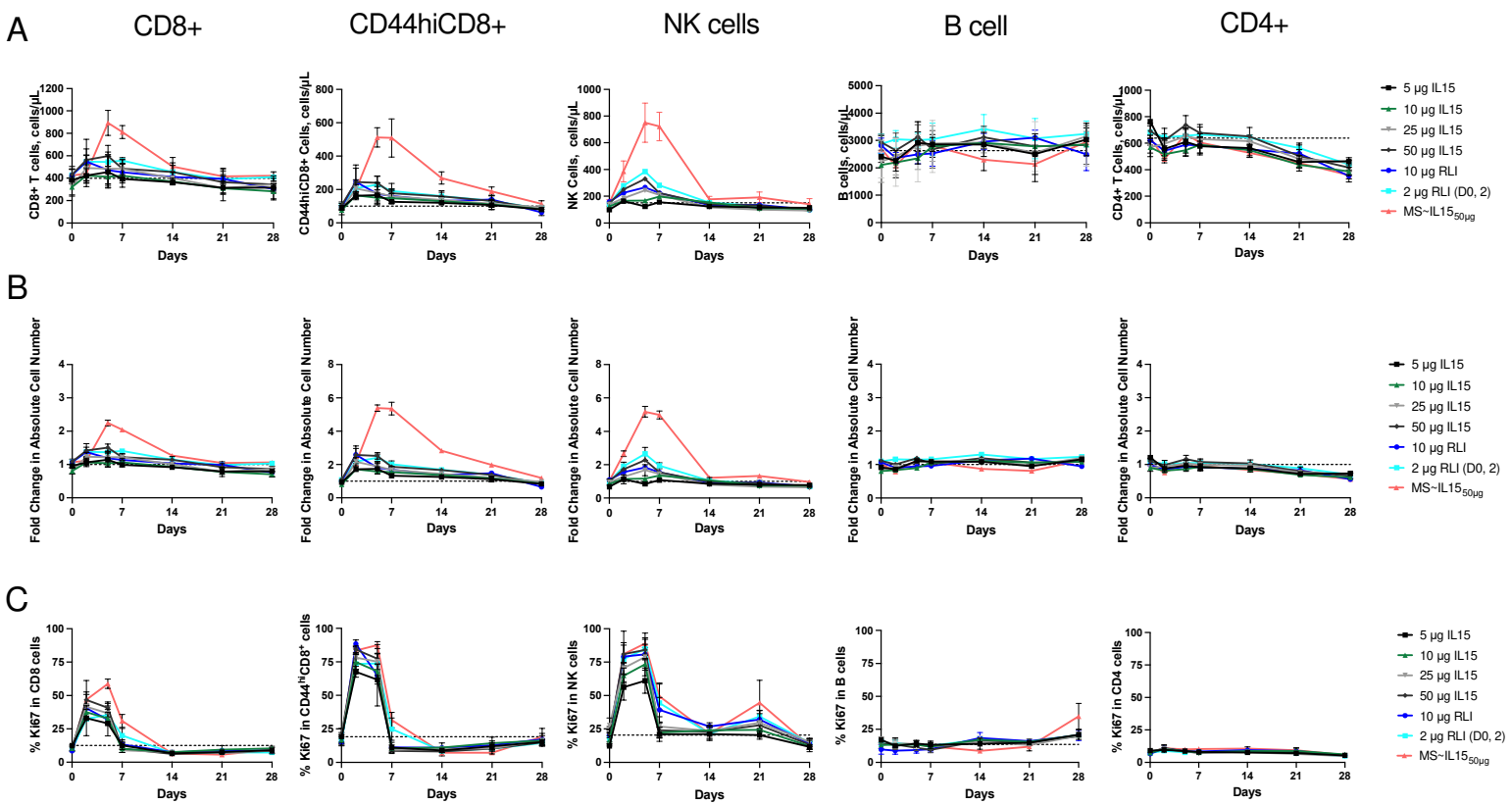

Figure S10. MS~IL-15$_{50µg}$ has significant increase in NK cells and CD44^{hi}CD8^{+} T cells compared to rhIL-15 and RLI. A) Absolute cell number B) Fold change in absolute cell number and C) Percentage of proliferating CD4^{+}, CD8^{+}, CD44^{hi}CD8^{+} , NK, and B cells. Mice were administered a single ip dose of rhIL-15 (5 – 50 µg), RLI (10 µg), two IP doses of RLI (2 µg) separated by 48 h, or a single SC dose of MS~IL-15$_{50µg}$ (n=4-5/group).

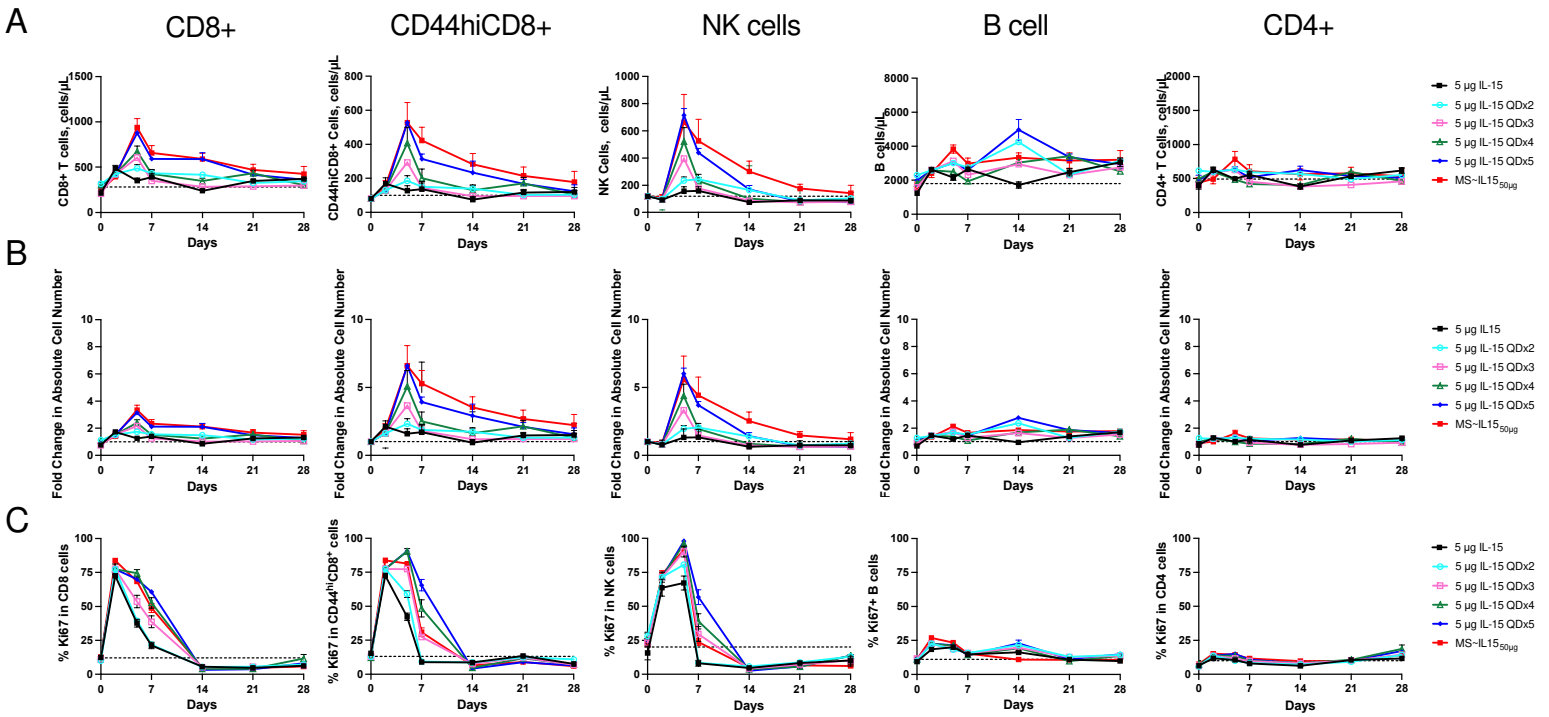

Figure S11. PD response of multiple doses of IL-15 compared to MS~IL-15$_{50µg}$. A) Absolute cell number B) Fold change in absolute cell number and C) Percentage of proliferating CD4^{+}, CD8^{+}, CD44^{hi}CD8^{+}, NK, and B cells. Mice were administered sequential daily IP doses of 5 µg rhIL-15 (QDx1 – QDx5) (n=5/group)

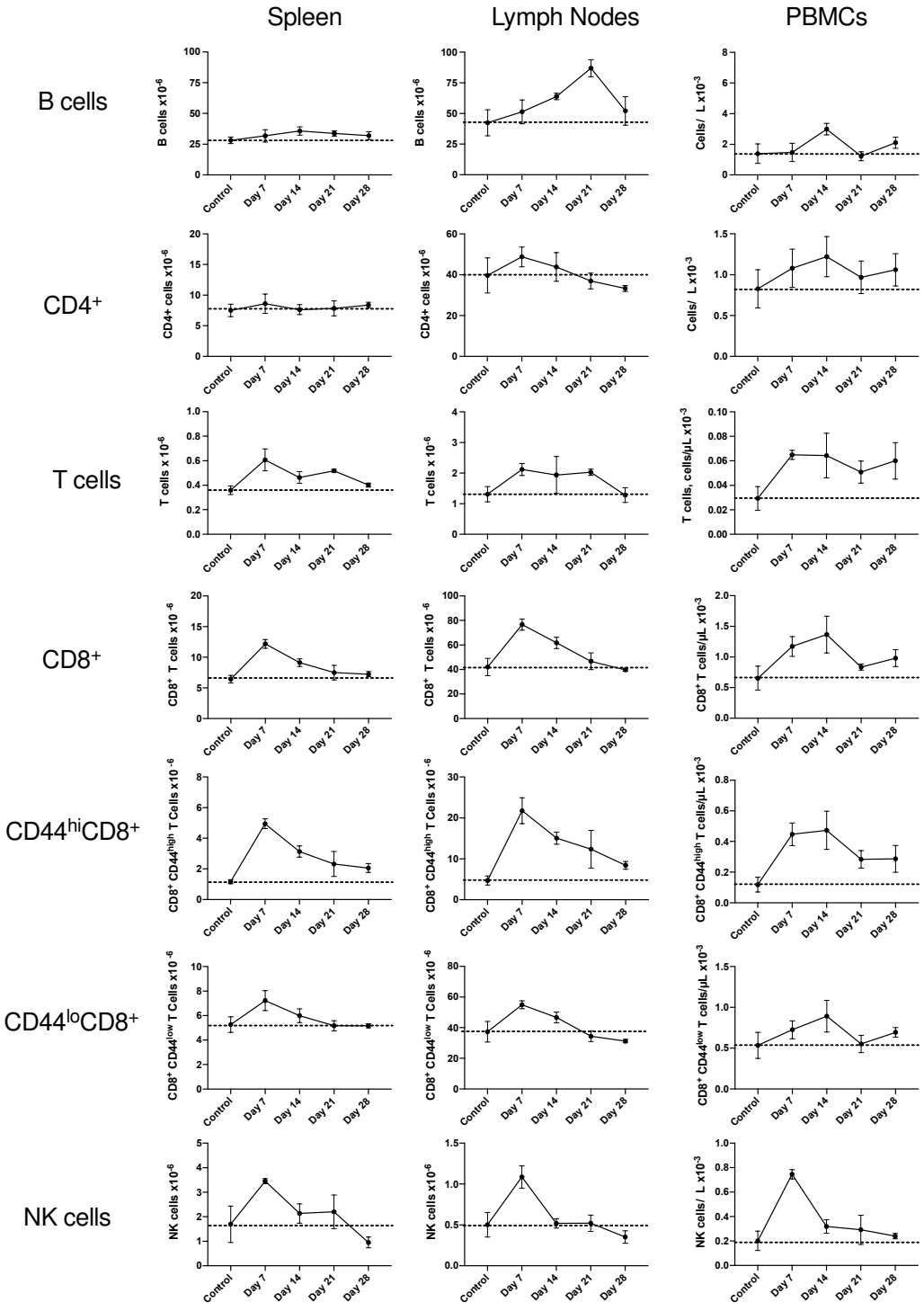
Spleen
Lymph Nodes
PBMCs
B cells
CD4+
T cells
CD8+
CD44hiCD8+
CD44loCD8+
NK cells
B cells x10-6
Cells/ L x10-3
CD4+ cells x10-6
T cells x 10-6
T cells, cells/µL x10-3
CD8+ T cells x10 -6
CD8+ T cells/µL x10-3
CD8+ CD44high T Cells x10 -6
CD8+ CD44high T cells/µL x10-3
CD8+ CD44low T Cells x10 -6
CD8+ CD44low T cells/µL x10-3
NK cells x10-6
NK cells/ L x10-3
Control
Day 7
Day 14
Day 21
Day 28

Figure S12. Absolute cell number immune cell expansion by MS_{GDM}~IL-$15_{50\mu g}$ measured over 28 d. Enumeration of B cells, NK cells, $CD4^+$, $CD8^+$, $CD44^{hi}CD8^+$, $CD44^{lo}CD8^+$and γδ T cells in the spleen, lymph nodes and blood of mice treated with 50 µg MS_{GDM}~IL-15. The dotted line represents the mean value of pre-treatment controls from 3 untreated mice. Tissues were collected (n=3 mice/time point) at 0, 7,14, 21 and 28 d and analyzed for specified cells.

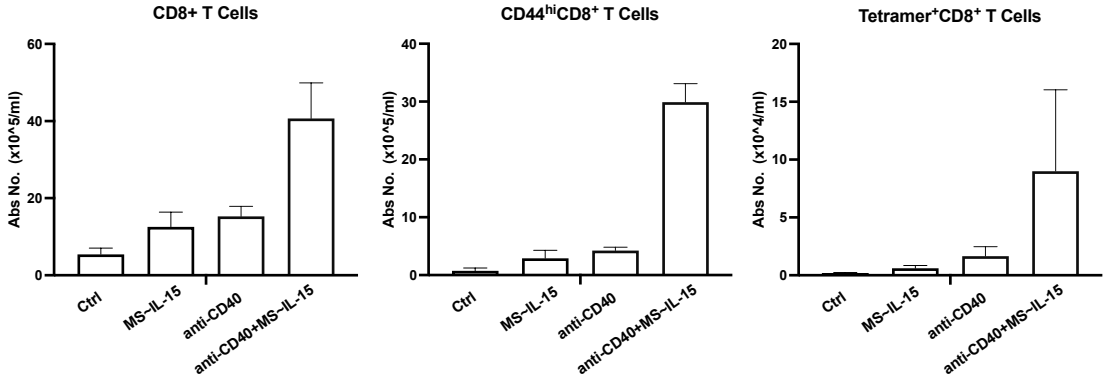

Figure S13. Absolute cell number CD8+ T cell expansion 16 days post treatment in C57BL/6J mice bearing TRAMP-C2 tumors on both flanks. Mice were treated with a single dose of SC MS~IL-$15_{50\mu g}$, IT anti-CD40 mAb (20 µg/10µl on d 0, 3, 7, and 10) in the right-flank tumor or the combination of MS~IL-$15_{50\mu g}$ plus anti-CD40. The control group was injected with PBS. Data represents average ± SD (n=2-4/group).

Table S2. AUC_{28d} for MS_{GDM}~IL-$15_{50\mu g}$ PD effect on target immune cells.

Marker	Tissue	pre-dose control, cells [A]	Duration, d	AUC, cells* d [B]
		mean ± SD		
$NK1.1^+$	spleen	1.7 ± 0.7	14	16
	ln	0.50 ± 0.15	14	3.8
	PBMC	0.18 ± 0.14	14	4.5
$CD8^+$	spleen	6.4 ± 0.62	21	69
	ln	42 ± 7	21	410
	PBMC	0.63 ± 0.18	21	11
$CD44^{hi}CD8^+$	spleen	1.2 ± 0.2	28	52
	ln	4.7 ± 1.1	28	260
	PBMC	0.11 ± 0.10	28	6.5
$TCR\gamma\delta^+$	spleen	0.36 ± 0.04	14	3.7
	ln	1.3 ± 0.2	28	15
	PBMC	0.03 ± 0.01	28	0.75

[A] Control values are cells * 10^{-6} for spleen and lymph nodes (ln), and cells/µl *10^{-3} for PBMCs.
[B] AUC values are cells * 10^{-6} * d for spleen and ln, and cells/µl *10^{-3} *d for PBMCs.

IX. Therapeutic studies of MS~IL15

TRAMP-C2 model. The TRAMP-C2 cell line, derived from a prostate tumor of the TRAMP mouse, was administered to four groups of wild-type C57 black mice on both flanks. When the tumors volumes reached 40-60 mm^3, treatment began. The treatment for each group was as follows: 1) empty microspheres, 2) anti-CD40 3) MS~$IL15_{50\mu g}$ 4) MS~$IL\text{-}15_{50\mu g}$ plus anti-CD40. Anti-CD40 (20 µg) was injected interlesionally in the right flank tumors on day 0, 3, 7 and 10. The impact on the time-course development of tumor size was determined for both the right side anti-CD40 injected and the left side untreated tumor. Kaplan-Meier mouse survival plots were generated based on the survival of mice in each group. The tumor size was measured in two orthogonal dimensions twice per week and survival of the mice was monitored throughout the experiment based on humane endpoint criteria. Tumor volume calculations were obtained from caliper measurements using the formula V = (W/2 x L/2).

Mouse Model of MET-1 leukemia. Six to eight-week-old female NOD.Cg-Prkdcscid/J mice (#001303) were purchased from the Jackson Laboratory (Bar Harbor, ME). MET-1 Leukemia was established by IP injection as previously described (*7*). Briefly, viably frozen or freshly isolated MET-1 from splenocytes ($2x10^7$ cells) was injected IP and the therapy was started when sIL-2Rα levels in mice serum were approximately 1,000 pg/ml which was 10–14 days after tumor inoculation. MS~$IL\text{-}15_{50\mu g}$ was injected on one occasion subcutaneously. CCR4 antibody (Mogamulizumab, 100 µg) was given via IP injection 2 days after MS~$IL\text{-}15_{50\mu g}$ injection and then weekly for 4 weeks alone or in combination with MS~$IL\text{-}15_{50\mu g}$ at the same dose and dosing schedule. The percentage and absolute number of NK cells were measured, and the survival of the mice was recorded.

X. Animal Welfare Statement

Animal experiments performed at the NIH/NCI were approved by the NCI Animal Care and Use Committee and were performed in accordance with NCI Animal Care and Use Committee guidelines. All other animal handling and care was performed by MuriGenics (Vallejo, CA) and Explora Biolabs (San Francisco, CA). All experiments conformed to IACUC recommendations.

XI. Derivation of Time Over Target Equation

For simple first-order clearance, the concentration of drug in the plasma at time t is given by:

$$C(t) = (Dose/V_d)\bullet exp(-k_e t)$$

where V_d = volume of distribution and k_e = the elimination rate constant. To calculate how long a given dose will provide plasma concentrations above a target concentration, C_{min} (i.e., the "time-over-target" = TOT):

$$C_{min} = (Dose/V_d)\bullet exp(-k_e t_{min})$$

$$TOT = t_{min} = [ln(Dose/(C_{min}\bullet V_d))]/k_e$$

Thus, there is a logarithmic relationship between dose and TOT:

$$TOT = A\bullet ln(Dose) - B$$

where A and B are constants determined by C_{min}, V_d, and k_e

$$A = 1/k_e$$

$$B = (ln(C_{min}\bullet V_d))/k_e$$

The change in time-over-target between two doses related as $Dose_2 = x\bullet Dose_1$ (i.e., an x-fold change in the dose) is thus given as

$$DTOT = TOT_2 - TOT_1 = A\bullet[ln(Dose_2) - ln(Dose_1)] = A\bullet ln(Dose_2/Dose_1)$$

$$DTOT = ln(x)/k_e = t_{1/2}\bullet ln(x)/ln(2)$$

The ratio of TOT_2/TOT_1 (i.e., the fold increase in TOT for a given fold increase in dose x) is thus

$$TOT_2/TOT_1 = (TOT_1 + DTOT)/TOT_1 = 1 + DTOT/TOT_1$$

Which simplifies to

$$TOT_2/TOT_1 = 1 + ln(x)/ln(Dose_1/C_{min}V_d)$$

If we are interested only in the relative fold-change in TOT with a certain fold-increase in dose X, this simplifies further to

$$TOT_2/TOT_1 = 1 + ln(x)/Z$$

$$\text{Where } Z = ln(Dose_1/C_{min}V_d)$$

XII. Supplemental discussion for the tolerance of MS~IL-15

The purpose of this study was to evaluate the toxicity/tolerability of MS~IL-15, when administered as subcutaneous (SC) injections on Day 1 and Day 15 to male C57BL/6 mice. Each treatment group (Groups 1–3) was comprised of six male C57BL/6 mice. Mice were administered the vehicle control (Group 1) or 0.15 or 0.50 mg/animal/injection MS~IL-15 (Groups 2 or 3, respectively) once on Day 1 (Injection Site #1) and once on Day 15 (Injection Site #2) via subcutaneous injection at a dose volume of 0.1 mL/injection. Clinical observations were recorded at least once daily, approximately 1 hour post-dose on dosing days, and on the day of necropsy. Physical examinations were conducted at randomization. Body weight measurements were taken for randomization, twice weekly, and prior to necropsy. Terminal plasma samples were collected from all groups at necropsy for bioanalysis of MS~IL-15. Blood samples for the evaluation of hematology and clinical chemistry endpoints were collected on Day 28 from all groups. Following blood sample collections, necropsy was conducted. Tissues were collected and evaluated grossly, select organs were weighed, and tissues were fixed for microscopic evaluation. Tissues were subsequently processed and evaluated microscopically.

All mice survived until the scheduled sacrifice. Compared to vehicle controls, there were no test article-related changes in body weights. There were no test article-related clinical pathology, organ weight, or macroscopic findings. Injection site swelling occurred across all groups with an overall exacerbated incidence following the second injection and a noteworthy increase in incidence at 0.50 mg/animal/injection, compared to vehicle controls, which persisted through Day 28. These changes were indicative of a vehicle-effect with test article exacerbation in MS~IL-15 groups.

At ≥0.15 mg/animal/injection, there was test article-related minimal to moderate subcutaneous granulomatous inflammation (Site 1, 0.15 mg/animal/injection - 4/6, 0.50 mg/animal/injection - 1/6, Site 2, 0.15 mg/animal/injection – 0/6, 0.50 mg/animal/injection - 1/6) that was not dose-dependent. All instances of test article-related granulomatous inflammation were associated with the microsphere vehicle. The identification of granulomatous inflammation in controls indicated that the microsphere vehicle contributed to inflammation to some degree. However, severity of inflammation was substantially higher in both Groups 2 and 3, which supported a test article-related effect. There was a single incidence of test article-related mild subcutaneous myofiber degeneration/regeneration at 0.15 mg/animal/injection.

In conclusion, MS~IL-15-related findings included minimal to moderate subcutaneous granulomatous inflammation (associated with the microsphere vehicle), one occurrence of mild myofiber degeneration/regeneration (0.15 mg/animal/injection only), and slight injection site swelling. Because there were no MS~IL-15 related changes in body weights and no dose-dependent microscopic differences between the 0.15 and 0.50 mg/animal/injection groups, MS~IL-15, administered every two weeks at 0.15 or 0.50 mg/animal/injection, was generally tolerated by male C57BL/6 mice, under the conditions of this study.

XIII. Supplemental References

1. K. C. Conlon, E. Lugli, H. C. Welles, S. A. Rosenberg, A. T. Fojo, J. C. Morris, T. A. Fleisher, S. P. Dubois, L. P. Perera, D. M. Stewart, C. K. Goldman, B. R. Bryant, J. M. Decker, J. Chen, T. A. Worthy, W. D. Figg, Sr., C. J. Peer, M. C. Sneller, H. C. Lane, J. L. Yovandich, S. P. Creekmore, M. Roederer, T. A. Waldmann, Redistribution, hyperproliferation, activation of natural killer cells and CD8 T cells, and cytokine production during first-in-human clinical trial of recombinant human interleukin-15 in patients with cancer. *J Clin Oncol* **33**, 74-82 (2015).
2. E. Mortier, A. Quemener, P. Vusio, I. Lorenzen, Y. Boublik, J. Grotzinger, A. Plet, Y. Jacques, Soluble interleukin-15 receptor alpha (IL-15R alpha)-sushi as a selective and potent agonist of IL-15 action through IL-15R beta/gamma. Hyperagonist IL-15 x IL-15R alpha fusion proteins. *J Biol Chem* **281**, 1612-1619 (2006).
3. H. Perdreau, E. Mortier, G. Bouchaud, V. Sole, Y. Boublik, A. Plet, Y. Jacques, Different dynamics of IL-15R activation following IL-15 cis- or trans-presentation. *Eur Cytokine Netw* **21**, 297-307 (2010).
4. D. F. Nellis, D. F. Michiel, M. S. Jiang, D. Esposito, R. Davis, H. Jiang, A. Korrell, G. C. t. Knapp, L. E. Lucernoni, R. E. Nelson, E. M. Pritt, L. V. Procter, M. Rogers, T. L. Sumpter, V. V. Vyas, T. J. Waybright, X. Yang, A. M. Zheng, J. L. Yovandich, J. A. Gilly, G. Mitra, J. Zhu, Characterization of recombinant human IL-15 deamidation and its practical elimination through substitution of asparagine 77. *Pharm Res* **29**, 722-738 (2012).
5. G. Soman, X. Yang, H. Jiang, S. Giardina, V. Vyas, G. Mitra, J. Yovandich, S. P. Creekmore, T. A. Waldmann, O. Quinones, W. G. Alvord, MTS dye based colorimetric CTLL-2 cell proliferation assay for product release and stability monitoring of interleukin-15: assay qualification, standardization and statistical analysis. *J Immunol Methods* **348**, 83-94 (2009).
6. E. L. Schneider, B. R. Hearn, S. J. Pfaff, S. D. Fontaine, R. Reid, G. W. Ashley, S. Grabulovski, V. Strassberger, L. Vogt, T. Jung, D. V. Santi, Approach for Half-Life Extension of Small Antibody Fragments That Does Not Affect Tissue Uptake. *Bioconjug Chem* **27**, 2534-2539 (2016).
7. K. E. Phillips, B. Herring, L. A. Wilson, M. S. Rickford, M. Zhang, C. K. Goldman, J. Y. Tso, T. A. Waldmann. IL-2Ralpha-Directed Monoclonal Antibodies Provide Effective Therapy in a Murine Model of Adult T-Cell Leukemia by a Mechanism other than Blockade of IL-2/IL-2Ralpha Interaction. *Cancer Research*. **60**, 6977-6984 (2000).